

Log-concave Density Estimation with Independent Components

Sharvaj Kubal, Christian Campbell, and Elina Robeva

Department of Mathematics, University of British Columbia

January 4, 2024

Abstract

We propose a method for estimating a log-concave density on \mathbb{R}^d from samples, under the assumption that there exists an orthogonal transformation that makes the components of the random vector independent. While log-concave density estimation is hard both computationally and statistically, the independent components assumption alleviates both issues, while still maintaining a large non-parametric class. We prove that under mild conditions, at most $\tilde{O}(\epsilon^{-4})$ samples (suppressing constants and log factors) suffice for our proposed estimator to be within ϵ of the original density in squared Hellinger distance. On the computational front, while the usual log-concave maximum likelihood estimate can be obtained via a finite-dimensional convex program, it is slow to compute – especially in higher dimensions. We demonstrate through numerical experiments that our estimator can be computed efficiently, making it more practical to use.

1 Introduction

A log-concave probability density p on \mathbb{R}^d is of the form $p(x) = e^{-\varphi(x)}$ for a closed, proper, convex function $\varphi : \mathbb{R}^d \rightarrow (-\infty, +\infty]$. Log-concave density estimation is a type of non-parametric density estimation dating back to the work of Walther [31]. The class of log-concave distributions includes many known parametric families, has attractive statistical properties, and admits maximum likelihood estimates (MLE) that can be computed with established optimization algorithms [28]. Moreover, the MLE is ‘automatic’ in that no tuning parameters (such as kernel bandwidths) need to be chosen – a feature that can be especially useful in higher dimensions. However, log-concave density estimation suffers from the curse of dimensionality – one requires $n \gtrsim_d \epsilon^{-\frac{d+1}{2}}$ samples (up to constants and log factors) for the log-concave MLE in \mathbb{R}^d to be ϵ close to the true density in squared Hellinger distance [22]. Furthermore, the log-concave MLE is too slow to compute for large values of d (e.g., $d \geq 6$ and $n \geq 5000$).

We reduce the family of log-concave densities by assuming that the components of the random vector at hand become independent after a suitable orthogonal transformation is applied – an *independent components* assumption. While the family that we study is somewhat restrictive, it includes all multivariate normal distributions, and is still non-parametric. Furthermore, the independent components assumption provides a link with independent component analysis (ICA) models, see [27]. We propose an easy-to-compute estimator for this family of densities and show that the sample complexity is no longer exponential in the ambient dimension d : with at most $n \gtrsim_d \epsilon^{-4}$ samples (up to constants and log factors), the estimate is within ϵ of the true density in squared Hellinger distance.

1.1 Prior work

Shape-constrained density estimation has a long history. Classes of shape-constrained densities that have previously been studied include non-increasing [15], convex [16], k -monotone [4], s -concave [12] and quasi-concave densities [20]. The log-concave class of densities was first studied in dimension 1 by Walther [31], and a concise description of the log-concave MLE in higher dimensions was given by Cule et al. [9]. Log-concavity has also gained popularity in applications [3; 28].

Subclasses of log-concave densities have also been studied in the recent years for the purposes of reducing the computational and statistical complexities of estimation, and also because they are important on their own. In the 1-dimensional setting, Kim et al. [18] study the set of log-concave densities that are

exponentials of concave functions defined by at most k linear hyperplanes. In this case, they show that the statistical rate becomes parametric. Robeva et al. [25] consider maximum likelihood estimation for totally positive and log-concave densities, which correspond to random vectors whose components are highly positively correlated. They prove existence and uniqueness of the MLE and propose an algorithm for computing it, although the statistical rates for this estimator are still unknown. Next, Kubjas et al. [21] study the family of log-concave densities that factorize according to an undirected graphical model, also providing existence and uniqueness results for the MLE (when the graph is given and chordal) together with an algorithm. Sample complexity rates for this model have not been studied either.

Here, we study the subfamily of log-concave densities on \mathbb{R}^d obtained by transforming product densities through orthogonal maps. These correspond to random vectors whose coordinates become independent post some orthogonal transformation. The most similar family to ours was considered by Samworth and Yuan [27], who study the class of log-concave densities of random vectors whose coordinates become independent after a linear transformation (rather than just an orthogonal transformation). They show that the projection (in a Kullback-Leibler (KL) sense) of a (not necessarily log-concave) distribution satisfying the above independent components property, to the set of log-concave distributions, still satisfies the independent components property with the same linear transformation. They also provide a method to perform density estimation in this setting, although their algorithm does not guarantee convergence to a global optimum. On the statistical front, they prove consistency; to the best of our knowledge however, finite sample rates have not yet been established in this setting. By simplifying the model here, we are able to provide a very fast algorithm together with sample complexity upper bounds that do not grow exponentially with the dimension.

Towards applicability to real data for tasks such as clustering, we show that our estimator can be used in conjunction with the Expectation-Maximization (EM) algorithm [11] to estimate mixtures of densities from our subfamily – this is a nonparametric generalization of Gaussian mixtures. A similar application was proposed in Cule et al. [9], where they show that mixtures of general log-concave densities can work better than Gaussian mixtures. However, estimating a mixture of general log-concave densities can be very costly, particularly in higher dimensions. Plugging our proposed estimator instead, into the EM algorithm, yields a much faster computation.

1.2 Problem

Suppose X is a zero-mean random vector in \mathbb{R}^d , with a (probability) density $p : \mathbb{R}^d \rightarrow \mathbb{R}$. Assume there exists an (unknown) orthogonal matrix $\mathbf{W} \in \mathbb{R}^{d \times d}$ such that the components of $Z = \mathbf{W}X$ are independent, and have log-concave densities. The joint density of Z , by assumption, can be written as

$$f(z) = \prod_{i=1}^d f_i(z_i), \quad (1)$$

where each $f_i : \mathbb{R} \rightarrow \mathbb{R}$ is a “1-dimensional” log-concave density. Our goal is to estimate the “ d -dimensional” density p of X from independent and identically distributed (iid) samples.

By writing $X = \mathbf{W}^{-1}Z$, we can interpret this as an independent component analysis (ICA) model, where Z is the vector of independent sources and \mathbf{W} is the so-called *unmixing matrix*. Although mixing matrices in ICA do not need to be orthogonal to begin with, a pre-whitening procedure [8] can transform the problem to such an orthogonal form.

Instead of estimating the d -dimensional density p directly, we would like to leverage the underlying structure provided by (1). This structure allows us to simplify p (using a change-of-variables formula) as

$$p(x) = \prod_{i=1}^d f_i([\mathbf{W}x]_i) = \prod_{i=1}^d f_i(w_i \cdot x), \quad (2)$$

where $w_i \in S^{d-1}$ is the i -th row of \mathbf{W} . We call (2) the *log-concave independent components* property for p , and refer to w_1, \dots, w_d as the *independent directions*. Note that the log-concavity of f_i for $i \in [d] := \{1, \dots, d\}$ is equivalent to imposing log-concavity upon p . Also note that the model $Z = \mathbf{W}X$ and the factorization in (2) are invariant under permuting the rows of \mathbf{W} and the corresponding components of Z , as well as under flipping their respective signs.

If \mathbf{W} is known beforehand – if it is provided by an *oracle* – the estimation problem is simplified, and one can use the following procedure:

1. Estimate the one-dimensional density f_i via log-concave maximum likelihood estimation [28], using the samples $\{Z_i^{(\ell)} = w_i \cdot X^{(\ell)} : \ell \in [N]\}$, where $X^{(1)}, \dots, X^{(N)} \stackrel{\text{iid}}{\sim} p$; denote the estimated density (MLE) by \hat{f}_i .
2. Plug-in the estimated densities into (2) to obtain the oracle-informed estimate of p :

$$\hat{p}_{\text{oracle}}(x) = \prod_{i=1}^d \hat{f}_i(w_i \cdot x) \quad (3)$$

In reality, the unmixing matrix \mathbf{W} is unknown, and one needs to estimate it. If the covariance matrix of X has distinct, well-separated eigenvalues, then this can be done by Principal Component Analysis (PCA), which involves diagonalizing the sample covariance matrix of X . Otherwise, a generalization – Fourier PCA [14] – may be used, provided certain non-Gaussianity requirements are satisfied. We refrain from using the same samples for the unmixing matrix estimation and the density estimation steps. Instead, we split the samples into two subsets, $\{X^{(1)}, \dots, X^{(N)}\}$ and $\{Y^{(1)}, \dots, Y^{(M)}\}$, and use different subsets for the two purposes in order to prevent potentially problematic cross-interactions. Further justification for this split and its role in our proof can be found in Section 2 and Appendix A.2.

Denote the (PCA or Fourier PCA) estimate of \mathbf{W} by $\hat{\mathbf{W}}$. Given enough samples, the rows $\hat{w}_1, \dots, \hat{w}_d$ of $\hat{\mathbf{W}}$ can be shown to be close to those of \mathbf{W} up to permutations and sign-flips. More precisely, there exists a permutation $\sigma : [d] \rightarrow [d]$ and signs $\theta_i \in \{-1, +1\}$ such that for some threshold $\epsilon > 0$

$$\|\hat{w}_i - \theta_i w_{\sigma(i)}\|_2 \leq \epsilon, \quad i \in [d].$$

As the factorization in (2) is invariant under such permutations and sign-flips, one can simply relabel $w_i \leftarrow \theta_i w_{\sigma(i)}$ and $Z_i \leftarrow \theta_i Z_{\sigma(i)}$ to proceed with the analysis.

From $\hat{\mathbf{W}}$, we can follow a procedure analogous to that used to obtain the oracle-informed estimate of p . Namely, we use the estimated independent directions $\hat{w}_i \in \mathbb{R}^d$ and the projected samples onto each such direction to produce one-dimensional estimates $\hat{p}_{\hat{w}_i}$; then we take the product of these estimates over i (see Definition 2.3).

1.3 Summary of contributions

The main contribution of this work is an algorithm for density estimation in the setting of Section 1.2, for which we prove finite sample guarantees and demonstrate numerical performance in terms of estimation errors and runtimes. The proposed algorithm is recorded as Algorithm 1.

The theoretical analysis in Section 3 yields sample complexity bounds for our algorithm, which are listed as corollaries in Section 3.4. Briefly, if the true density p satisfies some moment and smoothness assumptions in addition to the log-concave independent components property, then it can be estimated efficiently. In particular, $\text{poly}(d)/\epsilon^\varrho$ samples (up to log factors) where $\varrho \in [2, 4]$ are sufficient for our proposed estimator \hat{p} to be within ϵ of p in squared Hellinger distance with probability 0.99. The value of ϱ depends on the particular smoothness assumption being evoked, but is nevertheless bounded above by 4 regardless of the dimension d .

Since we rely on smoothness assumptions, a quick comparison with kernel density estimators (KDE) is in order. Recall that in dimension d , a KDE typically requires the true density p to have “smoothness of order d ” in order to achieve a dimension-independent statistical rate. More precisely, for p in the Sobolev space $\mathcal{W}^{s,1}(\mathbb{R}^d)$ with $s \geq 1$, achieving an expected total variation error of ϵ requires $n \gtrsim_d \epsilon^{-\frac{d+2s}{s}}$ samples [17] so that one needs $s \gtrsim d$ to counter the curse of dimensionality. On the contrary, our smoothness assumptions (see Smoothness assumption S1 and Smoothness assumption S2) are “order one” in that we only require control on the first-order (and if available, the second-order) derivatives.

Computational experiments are presented in Section 4, where we demonstrate improved estimation errors (in squared Hellinger distance) and improved runtimes as compared to usual log-concave MLE. A key consequence of our fast algorithm is easy scalability to higher dimensions – we are able to estimate densities in $d = 30$ within no more than a few seconds.

2 Set-up and algorithms

First, we establish some notation. For a random vector (e.g. X), the subscript labels the components of the vector in \mathbb{R}^d , whereas the superscript labels the iid samples (or copies). Given a (probability) density

$p : \mathbb{R}^d \rightarrow \mathbb{R}$ and a unit vector $s \in S^{d-1}$, define $p_s : \mathbb{R} \rightarrow \mathbb{R}$ to be the s -marginal of p . More precisely, if $X \sim p$, then $p_s = \text{Law}(s \cdot X)$. As described in Section 1, $Z = \mathbf{W}X$; similarly, define $\hat{Z} := \hat{\mathbf{W}}X$.

We denote by $\|\cdot\|_2$ the Euclidean norm on \mathbb{R}^d , and by $\|\cdot\|_{\text{op}}$ and $\|\cdot\|_F$ respectively the operator norm and the Frobenius norm on $\mathbb{R}^{d \times d}$. The squared Hellinger distance between densities $p, q : \mathbb{R}^d \rightarrow \mathbb{R}$ is defined as $h_d^2(p, q) = (1/2) \int_{\mathbb{R}^d} (\sqrt{q(x)} - \sqrt{p(x)})^2 dx = 1 - \int_{\mathbb{R}^d} \sqrt{q(x)p(x)} dx$. Note that $(p, q) \mapsto h_d(p, q) = \sqrt{h_d^2(p, q)}$ is a metric on the space of densities. Finally, for two quantities a and b , $a \lesssim b$ means that $a \leq Cb$ for some absolute constant $C > 0$ having no dependence on any parameters of the problem (including the dimension d).

Recall the zero-mean density p , satisfying the log-concave independent components property, and consider the split-up independent samples $\{X^{(1)}, \dots, X^{(N)}\}$ and $\{Y^{(1)}, \dots, Y^{(M)}\}$ as introduced in Section 1. Our procedure for estimating p consists of two stages: (1) use the samples $\{Y^{(1)}, \dots, Y^{(M)}\}$ to estimate the unmixing matrix \mathbf{W} , and (2) use the samples $\{X^{(1)}, \dots, X^{(N)}\}$ to estimate the marginal densities of p in the directions given by the (estimated) rows of \mathbf{W} . We expand on these below, starting with the unmixing matrix estimation.

For $X \sim p$, consider the covariance matrix $\Sigma = \mathbb{E}XX^T$. Since the components of $Z = \mathbf{W}X$ are independent, the covariance of Z

$$\Sigma_Z = \mathbb{E}ZZ^T = \mathbb{E}\mathbf{W}XX^T\mathbf{W}^T = \mathbf{W}\Sigma\mathbf{W}^T$$

is diagonal. Hence, the rows of \mathbf{W} are the (normalized) eigenvectors of Σ , and PCA can be used to estimate these eigenvectors under the following non-degeneracy condition:

Moment assumption M1 The eigenvalues of the covariance matrix $\Sigma = \mathbb{E}_{X \sim p}XX^T$ are separated from each other by at least $\delta > 0$.

From samples $Y^{(1)}, \dots, Y^{(M)} \stackrel{\text{iid}}{\sim} p$, one can compute the empirical covariance matrix

$$\hat{\Sigma} := \frac{1}{M} \sum_{j=1}^M Y^{(j)}Y^{(j)T}, \quad (4)$$

which is symmetric and positive semi-definite. Diagonalizing it yields the PCA-based estimate of \mathbf{W} .

Definition 2.1 (PCA-based estimate of \mathbf{W}). Let $Y^{(1)}, \dots, Y^{(M)} \stackrel{\text{iid}}{\sim} p$, and $\hat{\Sigma}$ defined as in (4). Denote by $\hat{w}_1, \dots, \hat{w}_d$ a set of orthonormal eigenvectors of $\hat{\Sigma}$. Then, the estimate $\hat{\mathbf{W}}$ is defined to be the orthogonal matrix whose rows are $\hat{w}_1, \dots, \hat{w}_d$.

Remark 2.2. Note that $\hat{\mathbf{W}}$ above is defined only up to permutations and sign-flips of the rows. This is consistent, nevertheless, with our earlier discussion on the invariance of the model with respect to these transformations.

By the concentration of $\hat{\Sigma}$ about Σ , and the Davis-Kahan theorem [30], the \hat{w}_i 's can be shown to be good estimates of w_i , provided δ is not too small (see Proposition 3.6).

Now consider the situation where the eigenvalues of Σ are poorly separated, or possibly degenerate. PCA may fail to recover the independent directions in this case. Consider, for example, the extreme case of an isotropic uniform distribution on a cube in \mathbb{R}^d with $\Sigma = \mathbf{I}$. Here, any $w \in S^{d-1}$ is an eigenvector of Σ , whereas the independent directions are only the d axes of the cube. When Σ has such degenerate eigenvalues, one needs to use higher moments to infer the unmixing matrix \mathbf{W} . An effective method with a polynomial sample complexity is Fourier-PCA [14], which requires the following assumptions on $Z = \mathbf{W}X$.

Moment assumption M2 For each $i \in [d]$, assume that the fourth moment $\mathbb{E}Z_i^4 \leq \mu_4$ for some $\mu_4 > 0$ and that there exists a $k_i \in \mathbb{N}$ (chosen as small as possible) such that the cumulant $|\text{cum}_{k_i}(Z_i)| \geq \Delta > 0$. Defining $k = \max_i k_i$, further assume that the corresponding k -th moments $\mathbb{E}|Z_i|^k \leq \mu_k$ for some $\mu_k > 0$.

Note that the assumption on the cumulants requires, in particular, that Z be non-Gaussian as is standard in ICA settings. Since \mathbf{W} is a square matrix, the simpler version of Fourier PCA based on diagonalizing a re-weighted covariance matrix suffices – see Goyal et al. [14, Algorithm 4]. The algorithm takes as input the samples $Y^{(1)}, \dots, Y^{(M)} \stackrel{\text{iid}}{\sim} p$ and the parameters Δ, k and μ_k from Moment assumption M2, and outputs an estimate $\hat{\mathbf{W}}$.

Given $\hat{\mathbf{W}}$, and hence the estimated independent directions $\hat{w}_1, \dots, \hat{w}_d$, consider the second stage of the estimation procedure now – estimating the marginal densities of p . Take the samples $X^{(1)}, \dots, X^{(N)} \stackrel{\text{iid}}{\sim} p$, which are independent from $Y^{(1)}, \dots, Y^{(M)}$, and project them as

$$\hat{Z}_i^{(j)} = \hat{w}_i \cdot X^{(j)}. \quad (5)$$

Conditional on $\hat{w}_1, \dots, \hat{w}_d$, it holds that

$$\hat{Z}_i^{(1)}, \dots, \hat{Z}_i^{(N)} \stackrel{\text{iid}}{\sim} p_{\hat{w}_i}$$

(almost surely in \hat{w}_i), which follows from the independence between \hat{w}_i and $X^{(j)}$. Log-concave MLE with $d = 1$ [31] can then be used to estimate each marginal $p_{\hat{w}_i}$ using the samples $\hat{Z}_i^{(1)}, \dots, \hat{Z}_i^{(N)}$. This procedure finally yields our proposed estimator.

Definition 2.3 (Proposed estimator). Let $X^{(1)}, \dots, X^{(N)} \stackrel{\text{iid}}{\sim} p$ be independent from $Y^{(1)}, \dots, Y^{(M)}$. For $\hat{w}_1, \dots, \hat{w}_d$ estimated as above, define the estimator

$$\hat{p}(x) = \prod_{i=1}^d \hat{p}_{\hat{w}_i}(\hat{w}_i \cdot x), \quad (6)$$

where $\hat{p}_{\hat{w}_i}$ is the log-concave MLE of $p_{\hat{w}_i}$ (conditional on \hat{w}_i).

Note that the proposed estimate is just the oracle-informed estimate with w_i replaced by \hat{w}_i (since $f_i = \text{Law}(Z_i) = p_{w_i}$). Further note that if we did not split the samples to conduct covariance estimation and density estimation separately, the law of \hat{Z}_i conditional on \hat{w}_i would no longer be $p_{\hat{w}_i}$; as a result, this proposed estimator would be somewhat ill-justified.

We can summarize the above discussion into an algorithm. Recall that we had assumed p to be zero-mean in our set-up; in the general case, one requires an additional centering step which we include below.

Algorithm 1 Log-concave independent components estimator (LC-IC)

- 1: Compute the empirical mean $\hat{\mu}$ and subtract it from the samples.
 - 2: Split the (centered) samples into two sets: $\{X^{(1)}, \dots, X^{(N)}\}$ and $\{Y^{(1)}, \dots, Y^{(M)}\}$.
 - 3: **if** Moment assumption M1 satisfied **then**
 - 4: $\hat{\mathbf{W}} := \text{PCAEstimate}(Y^{(1)}, \dots, Y^{(M)})$
 - 5: **else if** Moment assumption M2 satisfied **then**
 - 6: $\hat{\mathbf{W}} := \text{FourierPCAEstimate}(Y^{(1)}, \dots, Y^{(M)})$
 - 7: **end if**
 - 8: Compute $\hat{Z}^{(j)} := \hat{\mathbf{W}}X^{(j)}$ for $j = 1, \dots, N$.
 - 9: **for** $i \in \{1, \dots, d\}$ **do**
 - 10: $\hat{p}_{\hat{w}_i} := \text{LogConcaveMLE}(\hat{Z}_i^{(1)}, \dots, \hat{Z}_i^{(N)})$
 - 11: **end for**
 - 12: Compute $\hat{p}(x) := \prod_{i=1}^d \hat{p}_{\hat{w}_i}(\hat{w}_i \cdot x)$, where \hat{w}_i is the i -th row of $\hat{\mathbf{W}}$.
 - 13: Re-introduce the mean $\hat{\mu}$ to output $\hat{p}_{\hat{\mu}}(x) = \hat{p}(x - \hat{\mu})$.
-

Notice that we have not specified the sample splitting proportion between M and N . This is a free parameter in our method, and can be optimized based on the statistical rates obtained in Section 3.4, or based on numerical tests as explored in Section 4.2. An equal split with $M = N$ seems to generally work well. Finally, we use the R package `logcondens` [26] for the one-dimensional log-concave MLE step (Line 10) in Algorithm 1. This package also plays an important role in the computational speed of our method.

3 Analysis and sample complexities

This section is organized as follows. Section 3.1 presents some general, basic error bounds, allowing us to compare the proposed estimator with the oracle-informed estimator. Section 3.2 presents the sample complexity of estimating the unmixing matrix, and Section 3.3 provides a stability analysis under two different smoothness assumptions, aiming to quantify the effect of unmixing matrix estimation error on the proposed estimator. Finally, Section 3.4 gives the sample complexities of the proposed estimators as corollaries of the preceding analysis.

3.1 Basic error bounds

Throughout Section 3.1, let p be a probability density with mean zero, satisfying the log-concave independent components property (2). We analyse the oracle-informed estimator first.

Lemma 3.1. *Let \hat{p}_{oracle} be the oracle-informed estimator as defined in (3). We have the (tensorization) bound*

$$h_d^2(\hat{p}_{\text{oracle}}, p) = 1 - \prod_{i=1}^d (1 - h_1^2(\hat{p}_{w_i}, p_{w_i})) \leq d \max_{i \in [d]} h_1^2(\hat{p}_{w_i}, p_{w_i})$$

Proof. A direct calculation yields

$$1 - h_d^2(\hat{p}_{\text{oracle}}, p) = \int_{\mathbb{R}^d} \prod_{i=1}^d \sqrt{\hat{p}_{w_i}(w_i \cdot x) p_{w_i}(w_i \cdot x)} dx = \prod_{i=1}^d \int_{\mathbb{R}} \sqrt{\hat{p}_{w_i}(z_i) p_{w_i}(z_i)} dz_i = \prod_{i=1}^d (1 - h_1^2(\hat{p}_{w_i}, p_{w_i})).$$

Now define $b = \max_{i \in [d]} h_1^2(\hat{p}_{w_i}, p_{w_i})$ and note that $b \in [0, 1]$. Bernoulli's inequality gives that $\prod_{i=1}^d (1 - h_1^2(\hat{p}_{w_i}, p_{w_i})) \geq (1 - b)^d \geq 1 - db$. \square

Lemma 3.1 says that the problem of bounding $h_d^2(\hat{p}_{\text{oracle}}, p)$ boils down to controlling the one-dimensional log-concave estimation errors $h_1^2(\hat{p}_{w_i}, p_{w_i})$. Kim and Samworth [19] and Carpenter et al. [5] have already established results of this kind. Combining, we get the sample complexity of the oracle estimator.

Proposition 3.2 (Sample complexity of the oracle-informed estimator). *Let \hat{p}_{oracle} be the oracle-informed estimator computed from samples $X^{(1)}, \dots, X^{(N)} \stackrel{\text{iid}}{\sim} p$. Then, for any $\epsilon > 0$ and $0 < \gamma < 1$, we have*

$$h_d^2(\hat{p}_{\text{oracle}}, p) \leq \epsilon$$

with probability at least $1 - \gamma$, whenever

$$N \gtrsim \frac{d^2}{\epsilon^2} \log^6 \frac{d^2}{\epsilon \gamma}.$$

Proof. Define $\tilde{\epsilon} = \epsilon/d$ and $\tilde{\gamma} = \gamma/d$, so that

$$N \gtrsim \frac{1}{\tilde{\epsilon}^2} \log^6 \frac{1}{\tilde{\epsilon} \tilde{\gamma}}$$

Then, using Theorem 7 of Carpenter et al. [5] as applicable to the 1-dimensional log-concave MLE \hat{p}_{w_i} of p_{w_i} , computed from samples $Z_i^{(j)} = w_i \cdot X^{(j)}$ for $j = 1, \dots, N$, we get that $h_1^2(\hat{p}_{w_i}, p_{w_i}) \leq \tilde{\epsilon}$ holds with probability at least $1 - \tilde{\gamma}$ for any given $i \in [d]$. By a union bound, $\max_{i \in [d]} h_1^2(\hat{p}_{w_i}, p_{w_i}) \leq \tilde{\epsilon}$ with probability at least $1 - \tilde{\gamma}d = 1 - \gamma$. Finally, by Lemma 3.1,

$$h_d^2(\hat{p}_{\text{oracle}}, p) \leq \tilde{\epsilon}d = \epsilon.$$

\square

Having established an error bound for the oracle-informed estimator, we can now turn to our general setting. Here, we only have an estimate of \mathbf{W} , and hence, the estimation error needs to be taken into account. This contributes additional terms to the risk of the proposed estimator.

Theorem 3.3 (Error bound on the proposed estimator). *Let \hat{p} be the proposed estimator (Definition 2.3), computed from samples $X^{(1)}, \dots, X^{(N)}, Y^{(1)}, \dots, Y^{(M)} \stackrel{\text{iid}}{\sim} p$. We have the error bound*

$$h_d(\hat{p}, p) \leq \sqrt{d} \max_{i \in [d]} h_1(\hat{p}_{\hat{w}_i}, p_{\hat{w}_i}) + \sqrt{d} h_d(p \circ \hat{\mathbf{R}}^T, p) + h_d(p \circ \hat{\mathbf{R}}, p),$$

where $\hat{\mathbf{R}} = \mathbf{W}^T \hat{\mathbf{W}}$.

Proof. For $s \in S^{d-1}$, denote the projection $\pi_s(x) = s \cdot x$. This allows us to write the proposed estimator as

$$\hat{p}(x) = \prod_{i=1}^d \hat{p}_{\hat{w}_i}(\hat{w}_i \cdot x) = \prod_{i=1}^d \hat{p}_{\hat{w}_i} \circ \pi_{\hat{w}_i}(x). \quad (7)$$

We can break $h_d(\hat{p}, p)$ down into three terms that need to be controlled:

$$\begin{aligned} h_d(\hat{p}, p) &= h_d \left(\prod_i \hat{p}_{\hat{w}_i} \circ \pi_{\hat{w}_i}, \prod_i p_{w_i} \circ \pi_{w_i} \right) \\ &\leq h_d \left(\prod_i \hat{p}_{\hat{w}_i} \circ \pi_{\hat{w}_i}, \prod_i p_{\hat{w}_i} \circ \pi_{\hat{w}_i} \right) \\ &\quad + h_d \left(\prod_i p_{\hat{w}_i} \circ \pi_{\hat{w}_i}, \prod_i p_{w_i} \circ \pi_{w_i} \right) + h_d \left(\prod_i p_{w_i} \circ \pi_{w_i}, \prod_i p_{w_i} \circ \pi_{w_i} \right). \end{aligned} \quad (8)$$

This is essentially *removing hats* one-at-a-time. The first term is handled as

$$h_d^2 \left(\prod_i \hat{p}_{\hat{w}_i} \circ \pi_{\hat{w}_i}, \prod_i p_{\hat{w}_i} \circ \pi_{\hat{w}_i} \right) \leq d \max_{i \in [d]} h_1^2(\hat{p}_{\hat{w}_i}, p_{\hat{w}_i}), \quad (9)$$

using the simple tensorization argument from Lemma 3.1. Since $\prod_i p_{w_i} \circ \pi_{w_i}(x) = p(\hat{\mathbf{R}}x)$, we get that the third term equals $h_d(p \circ \hat{\mathbf{R}}, p)$.

Bounding the second term requires the following lemma.

Lemma 3.4. *Let p and w_1, \dots, w_d be defined as before, and consider any other probability density $q : \mathbb{R}^d \rightarrow \mathbb{R}$. Then,*

$$h_1^2(p_{w_k}, q_{w_k}) \leq h_d^2(p, q),$$

for $k \in [d]$.

The above lemma bounds the 1-dimensional Hellinger distance between marginals by the d -dimensional Hellinger distance between the full densities. This is a special case of the *data processing inequality* for f -divergences, but we nevertheless provide a proof in Appendix A.1. Noting that $p_{\hat{w}_k} = (p \circ \hat{\mathbf{R}}^T)_{w_k}$ and using Lemma 3.4 gives

$$h_1^2(p_{\hat{w}_i}, p_{w_i}) = h_1^2 \left((p \circ \hat{\mathbf{R}}^T)_{w_i}, p_{w_i} \right) \leq h_d^2 \left(p \circ \hat{\mathbf{R}}^T, p \right). \quad (10)$$

Now, to bound the second term, note that

$$\begin{aligned} 1 - h_d^2 \left(\prod_i p_{\hat{w}_i} \circ \pi_{\hat{w}_i}, \prod_i p_{w_i} \circ \pi_{w_i} \right) &= \int_{\mathbb{R}^d} \sqrt{\prod_i p_{\hat{w}_i}(\hat{w}_i \cdot x) p_{w_i}(\hat{w}_i \cdot x)} dx \\ &= \prod_i \int_{\mathbb{R}} \sqrt{p_{\hat{w}_i}(z'_i) p_{w_i}(z'_i)} dz'_i, \end{aligned}$$

via the change of variables $z' = \hat{\mathbf{W}}x$. The above expression can be lower bounded using (10):

$$\begin{aligned} \prod_i \int_{\mathbb{R}} \sqrt{p_{\hat{w}_i}(z'_i) p_{w_i}(z'_i)} dz'_i &= \prod_i (1 - h_1^2(p_{\hat{w}_i}, p_{w_i})) \geq \prod_i (1 - h_d^2(p \circ \hat{\mathbf{R}}^T, p)) \\ &= \left(1 - h_d^2(p \circ \hat{\mathbf{R}}^T, p) \right)^d \geq 1 - d \cdot h_d^2(p \circ \hat{\mathbf{R}}^T, p), \end{aligned}$$

where the last bound follows from Bernoulli's inequality. Hence,

$$h_d^2 \left(\prod_i p_{\hat{w}_i} \circ \pi_{\hat{w}_i}, \prod_i p_{w_i} \circ \pi_{w_i} \right) \leq d \cdot h_d^2(p \circ \hat{\mathbf{R}}^T, p),$$

which completes the last bit of the proof of Theorem 3.3. \square

The term $\max_{i \in [d]} h_1(\hat{p}_{\hat{w}_i}, p_{\hat{w}_i})$ in the bound of Theorem 3.3 warrants an analysis similar to the oracle-informed estimator. Since $\hat{p}_{\hat{w}_i}$ is the log-concave MLE of $p_{\hat{w}_i}$ conditional on \hat{w}_i , bounds on one-dimensional log-concave estimation [5; 19] control this term, when applied in a conditional sense.

Lemma 3.5 (Marginals of the proposed estimator). *Let p , \hat{p} , and \hat{w}_i as before. For any $0 < \epsilon < 1$ and $0 < \gamma < 1$, we have*

$$\max_{i \in [d]} h_1^2(\hat{p}_{\hat{w}_i}, p_{\hat{w}_i}) \leq \epsilon,$$

with probability at least $1 - \gamma$, whenever

$$N \gtrsim \frac{1}{\epsilon^2} \log^6 \frac{d}{\epsilon \gamma}.$$

The proof is deferred to Appendix A.2. To control the remaining terms from the bound of Theorem 3.3, we need the results from Section 3.2 and Section 3.3.

3.2 Unmixing matrix estimation

To proceed like in the case of the oracle estimator, we need to show closeness of \hat{w}_i and w_i . Recall that the methods used here for estimating \mathbf{W} – usual PCA or Fourier PCA – require different assumptions on the moments of X (or $Z = \mathbf{W}X$) in order to yield bounds on the estimation errors.

Consider regular PCA first. The PCA estimate of \mathbf{W} was obtained by computing the eigenvectors of the sample covariance matrix $\hat{\Sigma}$. Bounding the sample complexity of this estimation procedure is standard, and can be broken down into two simple steps: (i) bounding the distance between the empirical covariance matrix $\hat{\Sigma}$ and the true covariance matrix Σ , and (ii) bounding the distances between their corresponding eigenvectors. The result is summarized in the following proposition, the proof of which is delayed to Appendix A.3.

Proposition 3.6 (Sample complexity of estimating \mathbf{W} by PCA). *Let p be a zero-mean, log-concave probability density on \mathbb{R}^d . Let $Y^{(1)}, Y^{(2)}, \dots, Y^{(M)} \stackrel{\text{iid}}{\sim} p$ be samples, and suppose Moment assumption M1 is satisfied with eigenvalue separation $\delta > 0$. Let $\epsilon > 0$ and $0 < \gamma \leq 1/e$, and define $\tilde{M}(d, \gamma) := d \log^4(1/\gamma) \log^2(2 \log^2(1/\gamma))$. If*

$$M \gtrsim \tilde{M}(d, \gamma) \vee \left\{ \frac{\|\Sigma\|_{\text{op}}^2 d}{\delta^2 \epsilon^2} \log^4(1/\gamma) \log^2 \left(\frac{16 \|\Sigma\|_{\text{op}}^2}{\delta^2 \epsilon^2} \log^2(1/\gamma) \right) \right\},$$

then with probability at least $1 - \gamma$, PCA recovers vectors $\{\hat{w}_1, \dots, \hat{w}_d\}$ such that

$$\|\hat{w}_i - w_i\|_2 \leq \epsilon,$$

up to permutations and sign-flips.

Remark 3.7. The term $\tilde{M}(d, \gamma)$ is needed in order to allow the result above to hold for all positive ϵ , instead of just small values of ϵ .

Now, we consider the case of Fourier PCA; the theorem below is a restatement of Theorem 4.2 from Goyal et al. [14].

Theorem 3.8 (Sample complexity of estimating \mathbf{W} by Fourier PCA). *Let p be a zero-mean probability density on \mathbb{R}^d . Let $Y^{(1)}, Y^{(2)}, \dots, Y^{(M)} \stackrel{\text{iid}}{\sim} p$ be samples, and suppose the random vector $Z = \mathbf{W}Y$ for $Y \sim p$ satisfies Moment assumption M2 with parameters Δ, k, μ_4 , and μ_k . Given $\epsilon > 0$ and $0 < \gamma \leq 1/2$, if*

$$M \gtrsim (ckd)^{2k^2+2} \left(\frac{\mu_k}{\Delta} \right)^{2k+2} \frac{\mu_4^2}{\epsilon^2} \log(1/\gamma),$$

for an absolute constant $c > 0$, then with probability at least $1 - \gamma$, Fourier PCA recovers vectors $\{\hat{w}_1, \dots, \hat{w}_d\}$ such that

$$\|\hat{w}_i - w_i\|_2 \leq \epsilon,$$

up to permutations and sign-flips.

Remark 3.9. The bound in Theorem 4.2 of [14] holds with high probability. An arbitrarily high success probability of $1 - \gamma$ is achieved by *boosting* (see for example Lovász and Vempala [23, Theorem 2.8]), which is responsible for the additional factor of $\log 1/\gamma$ in the sample complexity above.

3.3 Stability in Hellinger distance

The second and third terms in the bound of Theorem 3.3 call for a notion of *stability*; $h_d(p \circ \hat{\mathbf{R}}, p)$ measures how far the rotated density $p \circ \hat{\mathbf{R}}$ gets from the original density p . If Hellinger distance is stable with respect to small rotations of the density, then $h_d(p \circ \hat{\mathbf{R}}, p)$ can be bounded effectively in terms of the operator norm $\|\mathbf{I} - \hat{\mathbf{R}}\|_{\text{op}}$, where \mathbf{I} is the $d \times d$ identity matrix. This operator norm is then well-controlled by the unmixing matrix estimation analysis from Section 3.2 as

$$\|\mathbf{I} - \hat{\mathbf{R}}\|_{\text{op}} = \|\mathbf{W} - \hat{\mathbf{W}}\|_{\text{op}} \leq \|\mathbf{W} - \hat{\mathbf{W}}\|_F = \sqrt{\sum_{i=1}^d \|\hat{w}_i - w_i\|_2^2} \leq \sqrt{d} \max_{i \in [d]} \|\hat{w}_i - w_i\|_2. \quad (11)$$

Stability in Hellinger distance depends crucially on the properties of the original density p – its smoothness in particular. In what follows, we consider two possible assumptions on the smoothness of p . The choice of assumptions then allows us to quantify stability in either Kullback-Leibler (KL) divergence or total variation distance first, before translating this to stability in Hellinger distance.

Let p be a probability density on \mathbb{R}^d with mean zero, and recall the associated covariance matrix $\boldsymbol{\Sigma}$. In the smoothness assumptions and stability results that follow throughout Section 3.3, we do *not* require p to be log-concave or satisfy the independent components property.

Smoothness assumption S1 The function $\varphi = -\log p$ is finite-valued everywhere, continuously differentiable, and belongs to the Hölder space $\mathcal{C}^{1,\alpha}(\mathbb{R}^d)$ for some $0 < \alpha \leq 1$, i.e.

$$[\nabla\varphi]_\alpha := \sup_{x \neq y} \frac{\|\nabla\varphi(y) - \nabla\varphi(x)\|_2}{\|y - x\|_2^\alpha} < \infty. \quad (12)$$

This assumption yields good stability in KL divergence, but it can be stringent since it requires, in particular, that p is strictly positive everywhere. The following assumption relaxes this.

Smoothness assumption S2 The density p has a (weak) gradient ∇p , with

$$\|\nabla p\|_{L^1} = \int_{\mathbb{R}^d} \|\nabla p(x)\|_2 dx < \infty. \quad (13)$$

This assumption yields a stability estimate in total variation distance (or equivalently, L^1 distance). Note that p is not required to be differentiable in the strong sense, and hence, can have “corners” or “kinks”. But, jumps are still not allowed. Also, to compare with assumption S1, note that if $p(x) = e^{-\varphi(x)}$ with $[\nabla\varphi]_\alpha < \infty$, then we write $\nabla p(x) = -\nabla\varphi(x)p(x)$ which can translate to a bound on $\|\nabla p\|_{L^1}$.

Assumptions S1 and S2 can be interpreted better by considering a multivariate Gaussian distribution with density

$$p(x) = a \exp\left(-\frac{1}{2}x \cdot \boldsymbol{\Sigma}^{-1}x\right)$$

where $a = (2\pi)^{-d/2}(\det \boldsymbol{\Sigma})^{-1/2}$ is the normalizing constant. Here, $\varphi(x) = \frac{1}{2}x \cdot \boldsymbol{\Sigma}^{-1}x - \log a$ is clearly $\mathcal{C}^{1,1}(\mathbb{R}^d)$, with $[\nabla\varphi]_1 = 1/\lambda_{\min}(\boldsymbol{\Sigma})$. On the other hand, $\|\nabla p\|_{L^1} \leq \sqrt{d/\lambda_{\min}(\boldsymbol{\Sigma})} < \infty$, provided $\lambda_{\min}(\boldsymbol{\Sigma}) > 0$. Now, we state our first stability theorem.

Theorem 3.10 (Stability in KL). *Let p be a zero-mean probability density on \mathbb{R}^d , satisfying Smoothness assumption S1. Let $\mathbf{R} \in \mathbb{R}^{d \times d}$ be any orthogonal matrix. Then,*

$$\text{KL}(p \| p \circ \mathbf{R}) \leq [\nabla\varphi]_\alpha d^{(1+\alpha)/2} \|\boldsymbol{\Sigma}\|_{\text{op}}^{(1+\alpha)/2} \|\mathbf{I} - \mathbf{R}\|_{\text{op}}^{1+\alpha}.$$

The proof involves a direct analysis of the KL integral, using the bound $\|\nabla\varphi(y) - \nabla\varphi(x)\|_2 \leq [\nabla\varphi]_\alpha \|y - x\|_2^\alpha$. It is delayed to Appendix A.4. This result translates to Hellinger distance via the upper bound [13]

$$h_d^2(p, p \circ \mathbf{R}) \leq \frac{1}{2} \text{KL}(p \| p \circ \mathbf{R}).$$

For the next stability result, we can go beyond rotations and consider more general linear maps on \mathbb{R}^d . Given a linear map $\mathbf{A} : \mathbb{R}^d \rightarrow \mathbb{R}^d$, denote by $\mathbf{A}_\# p$ the pushforward of p through \mathbf{A} , i.e. if $X \sim p$, then $\mathbf{A}X \sim \mathbf{A}_\# p$. Also, if \mathbf{A} is invertible, then $\mathbf{A}_\# p$ has the density $|\det(\mathbf{A}^{-1})| (p \circ \mathbf{A}^{-1})$, which simplifies to $p \circ \mathbf{A}^T$ when \mathbf{A} is orthogonal.

Theorem 3.11 (Stability in TV). *Let p be a zero-mean probability density on \mathbb{R}^d , satisfying Smoothness assumption S2. Let $\mathbf{A} \in \mathbb{R}^{d \times d}$ be invertible with $\|\mathbf{A}^{-1}\|_{\text{op}} \leq B$. Then,*

$$\text{TV}(p, \mathbf{A}_{\#}p) \equiv \frac{1}{2} \|\mathbf{A}_{\#}p - p\|_{L^1} \leq \frac{1}{2} \left[(1+B) \|\nabla p\|_{L^1} \sqrt{d} + d \right] \|\Sigma\|_{\text{op}}^{1/4} \|\mathbf{I} - \mathbf{A}\|_{\text{op}}^{1/2}.$$

The proof is based on bounding the Wasserstein-1 distance between p and $\mathbf{A}_{\#}p$, accompanied by an argument inspired from Chae and Walker [6] (see Appendix A.5). Again, the bound can be translated to Hellinger distance via the inequality [13]

$$h_d^2(p, \mathbf{A}_{\#}p) \leq \text{TV}(p, \mathbf{A}_{\#}p).$$

Finally, in the case of orthogonal matrices, the parameter $B = 1$.

3.4 Sample complexity results

Here, we present sample complexities of our algorithm as simple corollaries of the above bounds under the different moment and smoothness assumptions. Throughout Section 3.4, let p be a zero-mean probability density on \mathbb{R}^d , satisfying the log-concave independent components property, and let \hat{p} be the proposed estimator (Definition 2.3), computed from samples $X^{(1)}, \dots, X^{(N)}, Y^{(1)}, \dots, Y^{(M)} \stackrel{\text{iid}}{\sim} p$ as per Algorithm 1.

Corollary 3.12. *Suppose p satisfies Moment assumption M1 with $\delta > 0$, and Smoothness assumption S1 with $0 < \alpha \leq 1$. Let $\epsilon > 0$ and $0 < \gamma < 1/e$, and define $\tilde{M}(d, \gamma) := d \log^4(1/\gamma) \log^2(2 \log^2(1/\gamma))$. Then,*

$$h_d^2(\hat{p}, p) \leq \epsilon$$

with probability at least $1 - \gamma$, whenever

$$M \gtrsim \tilde{M}(d, \gamma) \vee \left\{ \frac{\|\Sigma\|_{\text{op}}^3 [\nabla \varphi]_{\alpha}^{\frac{2}{1+\alpha}} d^{\frac{5+3\alpha}{1+\alpha}}}{\delta^2 \epsilon^{\frac{2}{1+\alpha}}} \log^4(1/\gamma) \log^2 \left(\frac{\|\Sigma\|_{\text{op}}^3 [\nabla \varphi]_{\alpha}^{\frac{2}{1+\alpha}} d^{\frac{4+2\alpha}{1+\alpha}}}{\delta^2 \epsilon^{\frac{2}{1+\alpha}}} \log^2(1/\gamma) \right) \right\}, \quad (14a)$$

and

$$N \gtrsim \frac{d^2}{\epsilon^2} \log^6 \frac{d^2}{\epsilon \gamma}. \quad (14b)$$

Remark 3.13. Notice that we get a dependence of $1/\epsilon^{\frac{2}{1+\alpha}}$ in (14a), which is a better rate than $1/\epsilon^2$ for $\alpha > 0$.

Proof. Recall the decomposition

$$h_d(\hat{p}, p) \leq \sqrt{d} \max_{i \in [d]} h_1(\hat{p}_{\hat{w}_i}, p_{\hat{w}_i}) + \sqrt{d} h_d(p \circ \hat{\mathbf{R}}^T, p) + h_d(p \circ \hat{\mathbf{R}}, p),$$

from Theorem 3.3. By Lemma 3.5,

$$\sqrt{d} \max_{i \in [d]} h_1(\hat{p}_{\hat{w}_i}, p_{\hat{w}_i}) \leq \frac{\sqrt{\epsilon}}{2}$$

holds with probability at least $1 - \gamma/2$ provided (14b). On the other hand, by Theorem 3.10 and (11),

$$\begin{aligned} d \cdot h_d^2(p \circ \hat{\mathbf{R}}^T, p) &\leq \frac{1}{2} d \cdot \text{KL}(p \| p \circ \hat{\mathbf{R}}^T) \\ &\leq \frac{1}{2} d \cdot [\nabla \varphi]_{\alpha} d^{(1+\alpha)/2} \|\Sigma\|_{\text{op}}^{(1+\alpha)/2} \|\mathbf{I} - \hat{\mathbf{R}}^T\|_{\text{op}}^{1+\alpha} \\ &\leq \frac{1}{2} d^{2+\alpha} [\nabla \varphi]_{\alpha} \|\Sigma\|_{\text{op}}^{(1+\alpha)/2} \max_{i \in [d]} \|\hat{w}_i - w_i\|_2^{1+\alpha}, \end{aligned}$$

and similarly for the term $h_d^2(p \circ \hat{\mathbf{R}})$. The condition (14a) together with Proposition 3.6 then gives that

$$\sqrt{d} h_d(p \circ \hat{\mathbf{R}}^T, p) + h_d(p \circ \hat{\mathbf{R}}, p) \leq \frac{\sqrt{\epsilon}}{2}$$

with probability at least $1 - \gamma/2$. A final union bound then concludes the proof. \square

We now list the sample complexity corollaries under the remaining combinations of moment and smoothness assumptions. The proofs follow the same pattern as that of Corollary 3.12, and hence, are omitted.

Corollary 3.14. *Suppose p satisfies Moment assumption M1 with $\delta > 0$, and Smoothness assumption S2 with $\|\nabla p\|_{L^1} < \infty$. Let $\epsilon > 0$ and $0 < \gamma < 1/e$, and define $\tilde{M}(d, \gamma) := d \log^4(1/\gamma) \log^2(2 \log^2(1/\gamma))$. Then,*

$$h_d^2(\hat{p}, p) \leq \epsilon$$

with probability at least $1 - \gamma$, whenever

$$M \gtrsim \tilde{M}(d, \gamma) \vee \left\{ \frac{\|\Sigma\|_{\text{op}}^3 (\|\nabla p\|_{L^1}^4 d^8 + d^{10})}{\delta^2 \epsilon^4} \log^4(1/\gamma) \log^2 \left(\frac{\|\Sigma\|_{\text{op}}^3 (\|\nabla p\|_{L^1}^4 d^7 + d^9)}{\delta^2 \epsilon^4} \log^2(1/\gamma) \right) \right\}, \quad (15a)$$

and

$$N \gtrsim \frac{d^2}{\epsilon^2} \log^6 \frac{d^2}{\epsilon \gamma}. \quad (15b)$$

Notice that the requirement on N is the same as in Corollary 3.12, and this continues to hold for the remaining corollaries. On the other hand, possibly due to the weaker smoothness assumption, we get a worse dependence of $1/\epsilon^4$ in (15a).

Corollary 3.15. *Suppose p satisfies Moment assumption M2 with parameters Δ, k, μ_4, μ_k , and Smoothness assumption S1 with $0 < \alpha \leq 1$. For any $\epsilon > 0$ and $0 < \gamma < 1/2$, we have*

$$h_d^2(\hat{p}, p) \leq \epsilon$$

with probability at least $1 - \gamma$, whenever

$$M \gtrsim (ck)^{2k^2+2} \left(\frac{\mu_k}{\Delta} \right)^{2k+2} d^{2k^2+2+\frac{4+2\alpha}{1+\alpha}} \left(\frac{\|\Sigma\|_{\text{op}} \mu_4^2 [\nabla \varphi]_{\alpha}^{\frac{2}{1+\alpha}}}{\epsilon^{\frac{2}{1+\alpha}}} \right) \log(1/\gamma) \quad (16a)$$

for an absolute constant $c > 0$, and

$$N \gtrsim \frac{d^2}{\epsilon^2} \log^6 \frac{d^2}{\epsilon \gamma}. \quad (16b)$$

Corollary 3.16. *Suppose p satisfies Moment assumption M2 with parameters Δ, k, μ_4, μ_k , and Smoothness assumption S2 with $\|\nabla p\|_{L^1} < \infty$. For any $\epsilon > 0$ and $0 < \gamma < 1/2$, we have*

$$h_d^2(\hat{p}, p) \leq \epsilon$$

with probability at least $1 - \gamma$, whenever

$$M \gtrsim (ck)^{2k^2+2} \left(\frac{\mu_k}{\Delta} \right)^{2k+2} \left(\|\nabla p\|_{L^1}^4 d^{2k^2+9} + d^{2k^2+11} \right) \left(\frac{\|\Sigma\|_{\text{op}} \mu_4^2}{\epsilon^4} \right) \log(1/\gamma) \quad (17a)$$

for an absolute constant $c > 0$, and

$$N \gtrsim \frac{d^2}{\epsilon^2} \log^6 \frac{d^2}{\epsilon \gamma}. \quad (17b)$$

4 Computational experiments

In this section, we demonstrate the performance of the log-concave independent components estimator (LC-IC, Algorithm 1) on simulated as well as real data. Section 4.1 compares the estimation errors and runtimes of LC-IC with those of usual log-concave MLE on simulated multivariate normal data. Section 4.2 assesses the effect of the sample splitting proportions between the two tasks: estimation of \mathbf{W} (M samples) and estimation of the marginals (N samples). Finally, Section 4.3 combines LC-IC with the Expectation-Maximization (EM) algorithm [11] to estimate mixtures of densities from real data – the Wisconsin breast cancer dataset [32].

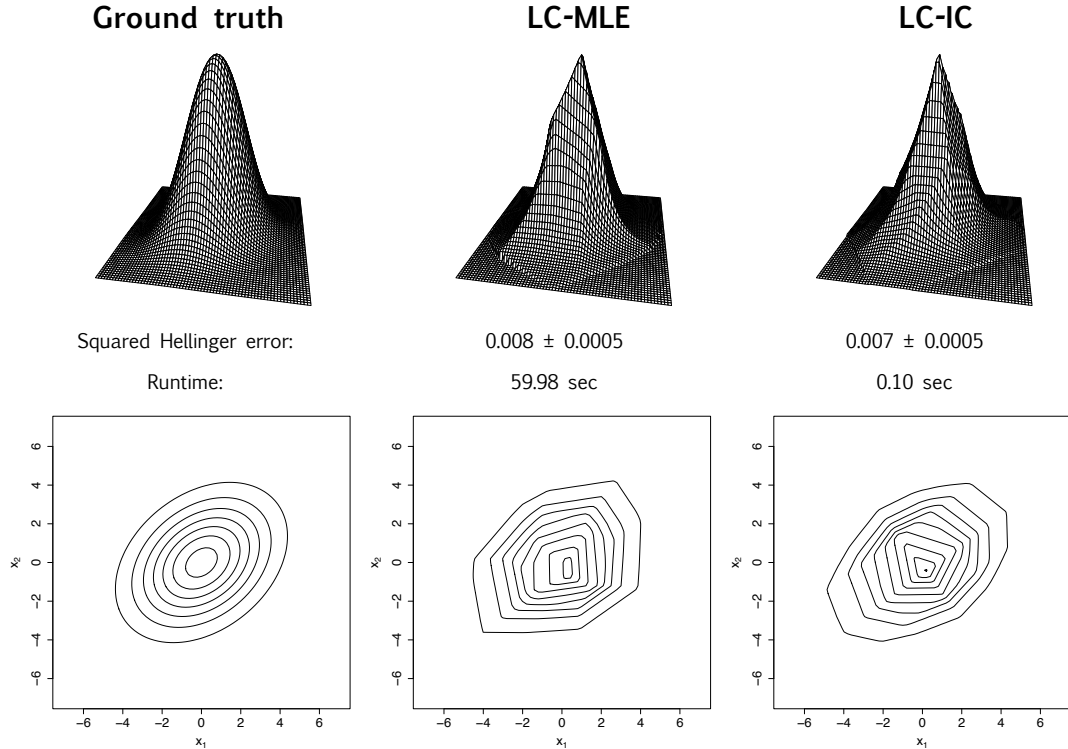


Figure 1: Comparing density estimation performance of our proposed log-concave independent components estimator (LC-IC) with the usual log-concave maximum likelihood estimator (LC-MLE), on simulated bivariate normal data. The ground truth and estimated densities are visualized in the top row, and the corresponding level curves are plotted in the bottom row.

4.1 Comparison of performance on simulated data

We first demonstrate estimation performance on bivariate normal data, and provide accompanying visualizations of the estimated density. Recalling that $X = \mathbf{W}^T Z$, we generate $Z \sim \mathcal{N}(0, \Sigma_Z)$ with $\Sigma_Z = \text{Diag}(6, 3)$, and choose the orthogonal matrix \mathbf{W} at random. With $n = 1000$ independent samples of X generated, we equally split $M = N = 500$, and compute the LC-IC estimate using PCA to estimate \mathbf{W} and `logcondens` to estimate the marginals. From the same $n = 1000$ samples, we also compute the usual log-concave maximum likelihood estimate (LC-MLE) using the R package `LogConcDEAD` [10]. Figure 1 shows the ground truth and estimated densities together with their contour plots, and lists the estimation errors in squared Hellinger distance along with the algorithm runtimes. The integrals needed to obtain the squared Hellinger distances are computed via a simple Monte-Carlo procedure (outlined in Appendix B.1); the associated uncertainty is also presented in Figure 1.

Table 1: Comparing average algorithm runtimes in **seconds** of our proposed log-concave independent components estimator (LC-IC) with the usual log-concave maximum likelihood estimator (LC-MLE), on simulated multivariate normal data. Here, n is the number of samples, and d is the dimension.

		$n = 100$	$n = 500$	$n = 1000$	$n = 2000$	$n = 3000$
$d = 2$	LC-MLE	0.56	11.93	60.79	469.65	1703.08
	LC-IC	0.02	0.04	0.10	0.09	0.12
$d = 3$	LC-MLE	1.82	42.00	141.31	874.58	3183.45
	LC-IC	0.02	0.06	0.08	0.13	0.17
$d = 4$	LC-MLE	8.70	155.03	735.06	4361.81	12933.45
	LC-IC	0.03	0.07	0.11	0.16	0.24

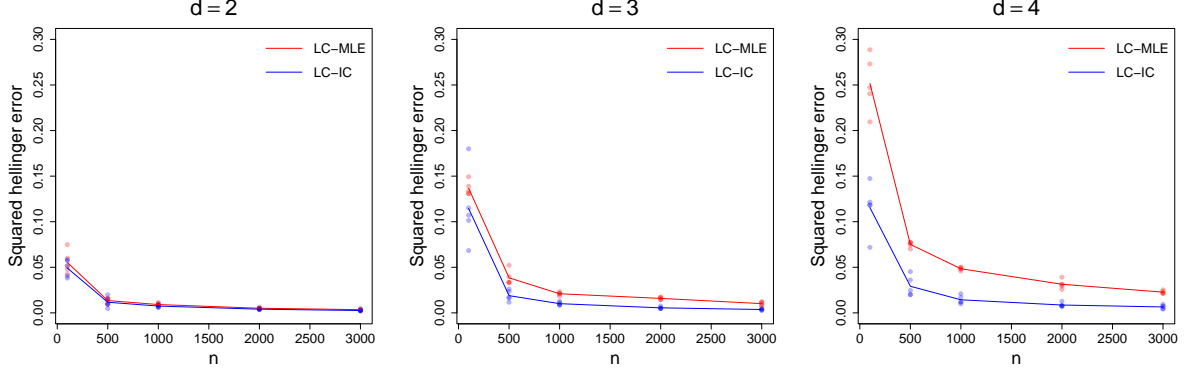


Figure 2: Comparing estimation errors in squared Hellinger distance of our proposed log-concave independent components estimator (LC-IC) with the usual log-concave maximum likelihood estimator (LC-MLE), on simulated multivariate normal data. The dots correspond to independent experiments, and the lines represent averages. Here, n is the number of samples, and d is the dimension.

Next, we conduct systematic comparison tests on simulated data from multivariate normal distributions in $d = 2, 3, 4$, with various values of n . As before, set $X = \mathbf{W}^T Z$ with \mathbf{W} chosen at random and $Z \sim \mathcal{N}(0, \Sigma_Z)$, where $\Sigma_Z = \text{Diag}(15, 14)$ for $d = 2$, $\Sigma_Z = \text{Diag}(15, 14, 13)$ for $d = 3$, and $\Sigma_Z = \text{Diag}(15, 14, 13, 12)$ for $d = 4$. PCA is used for estimating \mathbf{W} . Each experiment is repeated 5 times and the average metrics are presented. Algorithm runtime comparisons are given in Table 1, whereas the estimation errors in squared Hellinger distance are plotted in Figure 2. Notice that LC-IC runtimes are several orders of magnitude smaller than LC-MLE runtimes, especially for large n . Also, the estimation errors of LC-IC are lower than those of LC-MLE, with a growing margin as d increases.

Similar tests on Gamma-distributed data, are provided in Appendix B.3.

4.2 Effect of sample splitting proportions

We assess the effect of changing the sample splitting proportions between M and N on the estimation errors, for multivariate normal data in various dimensions. Using the total number of samples $n = M + N$, we define the parameter $r = M/n$ so that the extreme $r = 0$ corresponds to all samples being used for estimating the marginals, and $r = 1$ corresponds to all samples being used for estimating \mathbf{W} .

As before, $X = \mathbf{W}^T Z$ with the orthogonal matrix \mathbf{W} chosen at random and $Z \sim \mathcal{N}(0, \Sigma_Z)$, where for dimension $d \in \{2, 3, \dots, 9, 10, 15\}$ we set $\Sigma_Z = \text{Diag}(15, 14, \dots, 15 - (d - 1))$. With $n = 2000$ total samples, the values $r \in \{0.1, 0.2, \dots, 0.9\}$ are tested. PCA is used for estimating \mathbf{W} . Each experiment is

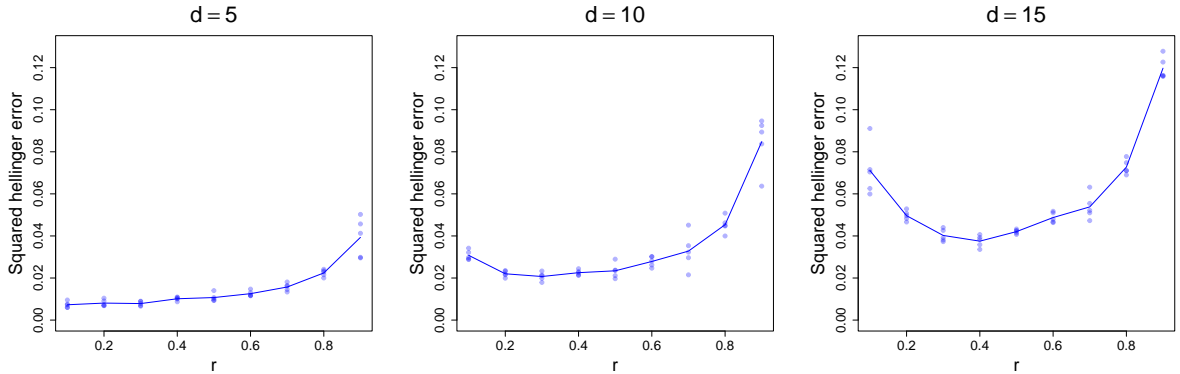


Figure 3: Demonstrating the effect of the sample splitting ratio $r = M/n$ on estimation error in squared Hellinger distance, for multivariate normal data in different dimensions d . The dots correspond to independent experiments, and the lines represent averages.

Table 2: Dependence of the error-minimizing sample splitting ratio r^* on dimension d for simulated multivariate normal data.

d	2	3	4	5	6	7	8	9	10	15
r^*	0.1	0.1	0.1	0.1	0.2	0.2	0.3	0.3	0.3	0.4

repeated 5 times independently, and the resulting estimation errors in squared Hellinger distance are presented in Figure 3 for $d = 5, 10, 15$.

Let r^* denote the minimizer of an r -versus-error curve for a fixed d , and notice that in Figure 3, r^* shifts to the right as d increases. This trend is tabulated for all values of d tested in Table 2. The observed shift is expected since the bounds for M (see (14a) in particular) have a stronger dependence on d compared to the bound for N (14b). However, we remark that the effect of d has not been completely isolated in the above experiment. The increase in d is accompanied by a corresponding decrease in $\lambda_{\min}(\Sigma)$, which worsens the smoothness of the density as discussed in Section 3.3. Keeping $\lambda_{\min}(\Sigma)$ fixed, on the other hand, would require shrinking the eigengap δ with d , but δ also appears in the bound (14a).

4.3 Estimating mixtures of densities and clustering

Consider the problem of estimating finite mixture densities of the form

$$p(x) = \sum_{k=1}^K \pi_k p_k(x), \quad (18)$$

where the mixture proportions π_1, \dots, π_k are nonnegative and sum to 1, and $p_1, \dots, p_k : \mathbb{R}^d \rightarrow \mathbb{R}$ are the component densities corresponding to different clusters. If the component densities are normal, the standard Gaussian EM (expectation maximization) algorithm can be used to estimate p . Chang and Walther [7] allowed for the component densities to be univariate log-concave by combining log-concave MLE with the EM algorithm. They also considered a normal copula for the multivariate case. This was later extended to general multivariate log-concave component densities by Cule et al. [9].

Here, we consider mixture densities of the form (18) where the component densities p_1, \dots, p_K (when centered to mean-zero positions) satisfy the log-concave independent components property. By combining the log-concave independent components estimator (LC-IC) with the EM algorithm, we can port the aforementioned computational benefits to this mixture setting.

We follow the general strategy in Cule et al. [9, Section 6.1], replacing their log-concave MLE step with LC-IC. Such a replacement is not completely obvious however. The log-concave MLE in this setting involves weighted samples, which are not immediately compatible with our sample splitting approach. Instead, we use a re-sampling heuristic as outlined in Appendix B.2.

Estimated mixture densities can be used for unsupervised clustering, and we test this on real data. To compare the performance of our EM + LC-IC against the results from Cule et al. [9, Section 6.2], we

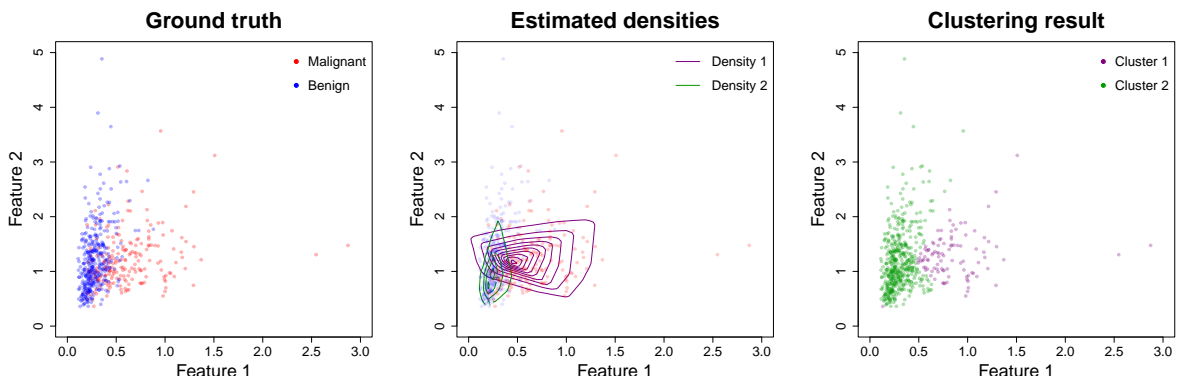


Figure 4: Estimating mixture densities and clustering using two features from the Wisconsin breast cancer dataset [32]. Labeling Cluster 1 as Malignant and Cluster 2 as Benign gives a 77.7% classification accuracy.

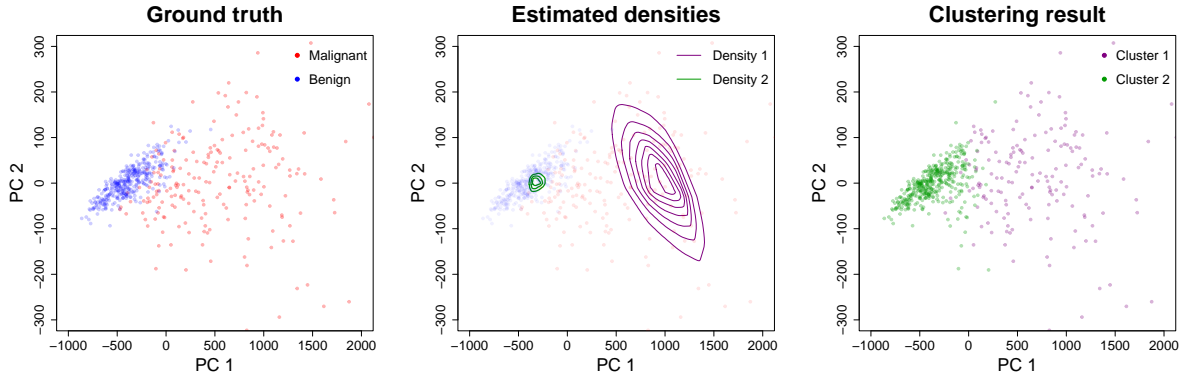


Figure 5: Estimating mixture densities and clustering using all 30 features from the Wisconsin breast cancer dataset [32]. The first two principal components are plotted. Labeling Cluster 1 as Malignant and Cluster 2 as Benign gives an 89.6% classification accuracy.

use the Wisconsin breast cancer dataset [32]. The dataset consists of 569 observations (individuals) and 30 features, where each observation is labeled with a diagnosis of *Malignant* or *Benign*. The test involves clustering the data without looking at the labels, and then comparing the learnt clusters with the ground truth labels.

First, we use the same two features as Cule et al. [9]: Feature 1 – standard error of the cell nucleus radius, and Feature 2 – standard error of the cell nucleus texture. This gives bivariate data ($d = 2$) with $n = 569$ samples. We employ EM + LC-IC with $K = 2$ target clusters, random initialization, and 20 EM iterations. Again, PCA is used for the \mathbf{W} -estimation steps. Figure 4 shows the data with ground truth labels (left-most plot), level curves of the estimated component densities (center plot), and the learnt clusters (right-most plot). Labeling Cluster 1 as Malignant and Cluster 2 as Benign attains a 77.7% classification accuracy (i.e. 77.7% of the instances are correctly labeled by the learnt clusters). This is close to the 78.7% accuracy reported in Cule et al. [9] (121 misclassified instances).

Next, we show improved clustering performance by using more features. Due to the scalability of LC-IC to higher dimensions, one can use all 30 features available in the dataset, so that $d = 30$. We employ EM + LC-IC with $K = 2$ target clusters as before, choose an initialization based on agglomerative hierarchical clustering (using the R package `mclust` [29]), and use 15 EM iterations. The results can be visualized in a PCA subspace of the data – the span of the two leading PCA eigenvectors (or loadings). This particular PCA is only used for visualization, and is *separate* from the PCA used in estimating \mathbf{W} .

Figure 5 shows the data in this PCA subspace with ground truth labels (left-most plot), level curves of the estimated component densities (center plot), and the learnt clusters (right-most plot). Labeling Cluster 1 as Malignant and Cluster 2 as Benign achieves an 89.6% classification accuracy, which is a significant improvement over the results for $d = 2$. In comparison, agglomerative hierarchical clustering on its own reaches an accuracy of 86.3%.

5 Discussion

We have looked at statistical and computational aspects of estimating densities satisfying the log-concave independent components property. First, we proved that up to $\text{poly}(d)/\epsilon^4$ iid samples (suppressing constants and log-factors) are sufficient for our proposed estimator \hat{p} to be ϵ -close to p with high confidence. Although squared Hellinger distance was used here, similar results could have been obtained for total variation (TV) distance since $\text{TV}(\hat{p}, p) \lesssim h_d(\hat{p}, p)$. Note that we do not claim these sample complexity bounds to be tight. The focus here was on demonstrating polynomial dependence on d , and it could certainly be possible for the power of d to be reduced further.

The results here could potentially be processed in the framework of Ashtiani et al. [2], who prove that any family of distributions admitting a so-called sample compression scheme can be learned with few samples. Furthermore, such compressibility extends to products and mixtures of that family. Hence, demonstrating sample compression in our setting would allow extending the sample complexities to mixtures of log-concave independent components densities, providing some theoretical backing to the

results from Section 4.3.

Next, the stability results from Section 3.3 could be of further theoretical interest, providing geometric insights into families of densities obtained from orthogonal or linear transformations of product densities. In particular, these could allow one to port covering and bracketing entropies from $d = 1$ to higher dimensions by discretizing the operator norm ball in $\mathbb{R}^{d \times d}$. Also note that these stability bounds are not necessarily tight – consider a spherically symmetric density q so that $h_d^2(q, q \circ \mathbf{R}) = 0$ for all orthogonal matrices \mathbf{R} . Our current analysis does not make use of such symmetry properties.

On the computational side, we showed that our algorithm has significantly smaller runtimes compared to usual log-concave MLE. This was achieved by breaking down the higher dimensional problem into several 1-dimensional ones. In fact these 1-dimensional marginal estimation tasks are decoupled from one another, allowing for effective parallelization to further reduce runtimes. Finally, we demonstrated the scalability of our algorithm by performing density estimation with clustering in $d = 30$.

Acknowledgement

Elina Robeva was supported by an NSERC Discovery Grant DGECR-2020-00338.

References

- [1] Radosław Adamczak, Alexander Litvak, Alain Pajor, and Nicole Tomczak-Jaegermann. Quantitative estimates of the convergence of the empirical covariance matrix in log-concave ensembles. *Journal of the American Mathematical Society*, 23(2):535–561, 2010.
- [2] Hassan Ashtiani, Shai Ben-David, Nicholas Harvey, Christopher Liaw, Abbas Mehrabian, and Yaniv Plan. Nearly tight sample complexity bounds for learning mixtures of gaussians via sample compression schemes. *Advances in Neural Information Processing Systems*, 31, 2018.
- [3] Mark Bagnoli and Ted Bergstrom. Log-concave probability and its applications. *Economic Theory*, 26(2):445–469, 2005.
- [4] Fadoua Balabdaoui and Jon A Wellner. Estimation of a k-monotone density: Limit distribution theory and the spline connection. *The Annals of Statistics*, 35(6):2536–2564, 2007.
- [5] Timothy Carpenter, Ilias Diakonikolas, Anastasios Sidiropoulos, and Alistair Stewart. Near-optimal sample complexity bounds for maximum likelihood estimation of multivariate log-concave densities. In *Conference On Learning Theory*, pages 1234–1262. PMLR, 2018.
- [6] Minwoo Chae and Stephen G. Walker. Wasserstein upper bounds of the total variation for smooth densities. *Statistics & Probability Letters*, 163:108771, 2020. ISSN 0167-7152.
- [7] George T Chang and Guenther Walther. Clustering with mixtures of log-concave distributions. *Computational Statistics & Data Analysis*, 51(12):6242–6251, 2007.
- [8] Pierre Comon and Christian Jutten. *Handbook of Blind Source Separation: Independent component analysis and applications*. Academic press, 2010.
- [9] Madeleine Cule, Richard Samworth, and Michael Stewart. Maximum likelihood estimation of a multi-dimensional log-concave density. *Journal of the Royal Statistical Society: Series B (Statistical Methodology)*, 72(5):545–607, 2010.
- [10] Madeleine Cule, Robert Gramacy, Richard Samworth, and Yining Chen. *LogConcDEAD: Log-Concave Density Estimation in Arbitrary Dimensions*, 2023. URL <https://CRAN.R-project.org/package=LogConcDEAD>. R package version 1.6-8.
- [11] Arthur P Dempster, Nan M Laird, and Donald B Rubin. Maximum likelihood from incomplete data via the em algorithm. *Journal of the royal statistical society: series B (methodological)*, 39(1):1–22, 1977.
- [12] Charles R Doss and Jon A Wellner. Global rates of convergence of the MLEs of log-concave and s-concave densities. *The Annals of Statistics*, 44(3):954, 2016.

- [13] Alison L Gibbs and Francis Edward Su. On choosing and bounding probability metrics. *International statistical review*, 70(3):419–435, 2002.
- [14] Navin Goyal, Santosh Vempala, and Ying Xiao. Fourier pca and robust tensor decomposition. In *Proceedings of the Forty-Sixth Annual ACM Symposium on Theory of Computing*, STOC '14, page 584–593, New York, NY, USA, 2014. Association for Computing Machinery. ISBN 9781450327107.
- [15] Ulf Grenander. On the theory of mortality measurement: Part ii. *Scandinavian Actuarial Journal*, 1956(2):125–153, 1956.
- [16] Piet Groeneboom, Geurt Jongbloed, and Jon A Wellner. Estimation of a convex function: Characterizations and asymptotic theory. *The Annals of Statistics*, 29(6):1653–1698, 2001.
- [17] Lasse Holmström and Jussi Klemelä. Asymptotic bounds for the expected l1 error of a multivariate kernel density estimator. *Journal of multivariate analysis*, 42(2):245–266, 1992.
- [18] Arlene K. Kim, Adityanand Guntuboyina, and Richard J. Samworth. Adaptation in log-concave density estimation. *The Annals of Statistics*, 46(5):2279 – 2306, 2018. doi: 10.1214/17-AOS1619.
- [19] Arlene KH Kim and Richard J Samworth. Global rates of convergence in log-concave density estimation. *The Annals of Statistics*, 44(6):2756–2779, 2016.
- [20] Roger Koenker and Ivan Mizera. Quasi-concave density estimation. *The Annals of Statistics*, 38(5): 2998–3027, 2010.
- [21] Kaie Kubjas, Olga Kuznetsova, Elina Robeva, Pardis Semnani, and Luca Sodomaco. Log-concave density estimation in undirected graphical models. *arXiv preprint arXiv:2206.05227*, 2022.
- [22] Gil Kur, Yuval Dagan, and Alexander Rakhlin. Optimality of maximum likelihood for log-concave density estimation and bounded convex regression. *arXiv:1903.05315*, 2019.
- [23] László Lovász and Santosh Vempala. The geometry of logconcave functions and sampling algorithms. *Random Structures & Algorithms*, 30(3):307–358, 2007. doi: <https://doi.org/10.1002/rsa.20135>.
- [24] Norman G. Meyers and James Serrin. $H = W$. *Proceedings of the National Academy of Sciences*, 51(6):1055–1056, 1964. doi: 10.1073/pnas.51.6.1055.
- [25] Elina Robeva, Bernd Sturmfels, Ngoc Tran, and Caroline Uhler. Maximum likelihood estimation for totally positive log-concave densities. *Scandinavian Journal of Statistics*, 48(3):817–844, 2021.
- [26] Kaspar Rufibach and Lutz Duembgen. *logcondens: Estimate a Log-Concave Probability Density from Iid Observations*, 2023. URL <https://CRAN.R-project.org/package=logcondens>. R package version 2.1.8.
- [27] Richard Samworth and Ming Yuan. Independent component analysis via nonparametric maximum likelihood estimation. *The Annals of Statistics*, 40(6):2973 – 3002, 2012. doi: 10.1214/12-AOS1060.
- [28] Richard J. Samworth. Recent Progress in Log-Concave Density Estimation. *Statistical Science*, 33(4):493 – 509, 2018. doi: 10.1214/18-STS666. URL <https://doi.org/10.1214/18-STS666>.
- [29] Luca Scrucca, Chris Fraley, T. Brendan Murphy, and Adrian E. Raftery. *Model-Based Clustering, Classification, and Density Estimation Using mclust in R*. Chapman and Hall/CRC, 2023. ISBN 978-1032234953. doi: 10.1201/9781003277965. URL <https://mclust-org.github.io/book/>.
- [30] Roman Vershynin. *High-dimensional probability: An introduction with applications in data science*, volume 47. Cambridge university press, 2018.
- [31] Guenther Walther. Detecting the presence of mixing with multiscale maximum likelihood. *Journal of the American Statistical Association*, 97(458):508–513, 2002.
- [32] William Wolberg, Olvi Mangasarian, Nick Street, and W. Street. Breast Cancer Wisconsin (Diagnostic). UCI Machine Learning Repository, 1995. DOI: <https://doi.org/10.24432/C5DW2B>.

A Delayed proofs

A.1 Proof of Lemma 3.4

Lemma. Let p and w_1, \dots, w_d as before, and consider any other probability density $q : \mathbb{R}^d \rightarrow \mathbb{R}$. Then,

$$h_1^2(p_{w_k}, q_{w_k}) \leq h_d^2(p, q),$$

for $k \in [d]$.

Proof. Writing

$$1 - h_d^2(p, q) = \int_{\mathbb{R}^d} \sqrt{p(x)q(x)} dx = \int_{\mathbb{R}^d} \sqrt{\prod_i p_{w_i}(w_i \cdot x) q(x)} dx,$$

and changing variables $z = \mathbf{W}x$ gives

$$\int_{\mathbb{R}^d} \sqrt{\prod_i p_{w_i}(z_i) \bar{q}(z)} dz,$$

where $\bar{q}(z) := q(\mathbf{W}^T z)$. Splitting the components of z as z_k and $z_{[d] \setminus k}$ allows us to rewrite the above expression as an iterated integral, and use Cauchy-Schwarz on the inner integral:

$$\begin{aligned} & \int_{\mathbb{R}} \int_{\mathbb{R}^{d-1}} \sqrt{\prod_{i \neq k} p_{w_i}(z_i) \bar{q}(z_k, z_{[d] \setminus k})} dz_{[d] \setminus k} \sqrt{p_{w_k}(z_k)} dz_k \\ & \leq \int_{\mathbb{R}} \left\{ \int_{\mathbb{R}^{d-1}} \prod_{i \neq k} p_{w_i}(z_i) dz_{[d] \setminus k} \right\}^{1/2} \left\{ \int_{\mathbb{R}^{d-1}} \bar{q}(z_k, z_{[d] \setminus k}) dz_{[d] \setminus k} \right\}^{1/2} \sqrt{p_{w_k}(z_k)} dz_k. \end{aligned}$$

Since each p_i is a probability density,

$$\int_{\mathbb{R}^{d-1}} \prod_{i \neq k} p_{w_i}(z_i) dz_{[d] \setminus k} = \prod_{i \neq k} \int_{\mathbb{R}} p_{w_i}(z_i) dz_i = 1.$$

On the other hand, \bar{q} is being marginalized and

$$\bar{q}_{e_k}(z_k) := \int_{\mathbb{R}^{d-1}} \bar{q}(z_k, z_{[d] \setminus k}) dz_{[d] \setminus k}$$

is the marginal of \bar{q} along the direction e_k . Noting that $\bar{q}_{e_k} = q_{w_k}$ and chaining together the above inequalities gives the desired result:

$$1 - h_d^2(p, q) \leq \int_{\mathbb{R}} \sqrt{q_{w_k}(z_k) p_{w_k}(z_k)} dz_k = 1 - h_1^2(p_{w_k}, q_{w_k}).$$

□

A.2 Proof of Lemma 3.5

Lemma. Let p, \hat{p} , and \hat{w}_i as before. For any $0 < \epsilon < 1$ and $0 < \gamma < 1$, we have

$$\max_{i \in [d]} h_1^2(\hat{p}_{\hat{w}_i}, p_{\hat{w}_i}) \leq \epsilon,$$

with probability at least $1 - \gamma$, whenever

$$N \gtrsim \frac{1}{\epsilon^2} \log^6 \frac{d}{\epsilon \gamma}.$$

Proof. The estimate $\hat{p}_{\hat{w}_i}$ is computed from the projected samples $\hat{Z}_i^{(j)} = \hat{w}_i \cdot X^{(j)}$, where conditional on $\hat{w}_1, \dots, \hat{w}_d$, it holds that

$$\hat{Z}_i^{(1)}, \dots, \hat{Z}_i^{(N)} \stackrel{\text{iid}}{\sim} p_{\hat{w}_i}$$

(almost surely in \hat{w}_i). As $\hat{p}_{\hat{w}_i}$ is the log-concave MLE of $p_{\hat{w}_i}$ conditional on \hat{w}_i , we have from Carpenter et al. [5, Theorem 7] that

$$\mathbb{P} \left\{ h_1^2(\hat{p}_{\hat{w}_i}, p_{\hat{w}_i}) > \epsilon \mid \hat{w}_i \right\} \leq \frac{\gamma}{d}$$

almost surely in \hat{w}_i provided

$$N \gtrsim \frac{1}{\epsilon^2} \log^6 \frac{d}{\epsilon \gamma}.$$

Taking expectation with respect to the randomness in \hat{w}_i yields the same inequality for the unconditional probability:

$$\begin{aligned} \mathbb{P} \left\{ h_1^2(\hat{p}_{\hat{w}_i}, p_{\hat{w}_i}) > \epsilon \right\} &= \mathbb{E} \mathbf{1} \left\{ h_1^2(\hat{p}_{\hat{w}_i}, p_{\hat{w}_i}) > \epsilon \right\} = \mathbb{E}_{\hat{w}_i} \mathbb{E} \left[\mathbf{1} \left\{ h_1^2(\hat{p}_{\hat{w}_i}, p_{\hat{w}_i}) > \epsilon \right\} \mid \hat{w}_i \right] \\ &= \mathbb{E}_{\hat{w}_i} \mathbb{P} \left\{ h_1^2(\hat{p}_{\hat{w}_i}, p_{\hat{w}_i}) > \epsilon \mid \hat{w}_i \right\} \leq \frac{\gamma}{d}. \end{aligned}$$

Combining this with a union bound over $i \in [d]$ gives that

$$\max_{i \in [d]} h_1^2(\hat{p}_{\hat{w}_i}, p_{\hat{w}_i}) \leq \epsilon$$

with probability at least $1 - \gamma$. □

A.3 Proof of Proposition 3.6

Proposition. (Sample complexity of estimating \mathbf{W} by PCA) Let p be a zero-mean, log-concave probability density on \mathbb{R}^d . Let $Y^{(1)}, Y^{(2)}, \dots, Y^{(M)} \stackrel{\text{iid}}{\sim} p$ be samples, and suppose Moment assumption M1 is satisfied with eigenvalue separation $\delta > 0$. Let $\epsilon > 0$ and $0 < \gamma \leq 1/e$, and define $\tilde{M}(d, \gamma) := d \log^4(1/\gamma) \log^2(2 \log^2(1/\gamma))$. If

$$M \gtrsim \tilde{M}(d, \gamma) \vee \left\{ \frac{\|\Sigma\|_{\text{op}}^2 d}{\delta^2 \epsilon^2} \log^4(1/\gamma) \log^2 \left(\frac{16 \|\Sigma\|_{\text{op}}^2}{\delta^2 \epsilon^2} \log^2(1/\gamma) \right) \right\},$$

then with probability at least $1 - \gamma$, PCA recovers vectors $\{\hat{w}_1, \dots, \hat{w}_d\}$ such that

$$\|\hat{w}_i - w_i\|_2 \leq \epsilon,$$

up to permutations and sign-flips.

Proof. Since w_i and \hat{w}_i are eigenvectors of Σ and $\hat{\Sigma}$ respectively, Davis-Kahan theorem [30, Theorem 4.5.5] gives the bound

$$\|\hat{w}_i - w_i\|_2 \leq \frac{2^{3/2}}{\delta} \|\hat{\Sigma} - \Sigma\|_{\text{op}},$$

for some permutation and choice of sign-flips of w_1, \dots, w_d . Hence, the problem boils down to covariance estimation of log-concave random vectors [1].

To bring the problem into an isotropic setting, define random vectors $V^{(j)} := \Sigma^{-1/2} Y^{(j)}$ for $j = 1, \dots, M$, such that $\mathbb{E} V^{(j)} V^{(j)T} = \mathbf{I}$, and note that these still have log-concave densities. By Theorem 4.1 of Adamczak et al. [1], for any $\tilde{\epsilon} \in (0, 1)$ and $t \geq 1$, if

$$M \gtrsim d \frac{t^4}{\tilde{\epsilon}^2} \log^2 \left(\frac{2t^2}{\tilde{\epsilon}^2} \right),$$

then with probability at least $1 - e^{-ct\sqrt{d}}$ where $c > 0$ is an absolute constant, it holds that

$$\left\| \frac{1}{M} \sum_{j=1}^M V^{(j)} V^{(j)T} - \mathbf{I} \right\|_{\text{op}} \leq \tilde{\epsilon}. \quad (19)$$

For a $\gamma \in (0, 1/e]$, we have $\log(1/\gamma) \geq 1$ so that setting $t = C \log(1/\gamma)$ for a large enough absolute constant $C > 0$ results in the failure probability being bounded above as $e^{-ct\sqrt{d}} \leq \gamma$. Hence, (19) holds with probability at least $1 - \gamma$, provided

$$M \gtrsim \frac{d}{\tilde{\epsilon}^2} \log^4(1/\gamma) \log^2 \left(\frac{2}{\tilde{\epsilon}^2} \log^2(1/\gamma) \right).$$

Furthermore, letting $\tilde{\epsilon} \uparrow 1$ yields that

$$\left\| \frac{1}{M} \sum_{j=1}^M V^{(j)} V^{(j)T} - \mathbf{I} \right\|_{\text{op}} \leq 1$$

with probability at least $1 - \gamma$ provided $M \gtrsim \tilde{M}(d, \gamma)$. As a result, (19) also extends to $\tilde{\epsilon} \geq 1$. Finally, letting $\tilde{\epsilon} = 2^{-3/2} \epsilon \delta \|\Sigma\|_{\text{op}}^{-1}$ gives the required result, since

$$\begin{aligned} \|\hat{\Sigma} - \Sigma\|_{\text{op}} &= \left\| \frac{1}{M} \sum_{j=1}^M Y^{(j)} Y^{(j)T} - \Sigma \right\|_{\text{op}} \\ &= \left\| \Sigma^{1/2} \left(\frac{1}{M} \sum_{j=1}^M V^{(j)} V^{(j)T} - \mathbf{I} \right) \Sigma^{1/2} \right\|_{\text{op}} \\ &\leq \|\Sigma\|_{\text{op}} \tilde{\epsilon} \leq \frac{\delta}{2^{3/2}} \epsilon. \end{aligned}$$

□

A.4 Proof of Theorem 3.10

Theorem. Let p be a zero-mean probability density on \mathbb{R}^d , satisfying Smoothness assumption S1. Let $\mathbf{R} \in \mathbb{R}^{d \times d}$ be any orthogonal matrix. Then,

$$\text{KL}(p \| p \circ \mathbf{R}) \leq [\nabla \varphi]_{\alpha} d^{(1+\alpha)/2} \|\Sigma\|_{\text{op}}^{(1+\alpha)/2} \|\mathbf{I} - \mathbf{R}\|_{\text{op}}^{1+\alpha}.$$

Proof. Recall the KL divergence

$$\begin{aligned} \text{KL}(p \| p \circ \mathbf{R}) &= \int_{\mathbb{R}^d} p(x) (\log p(x) - \log p(\mathbf{R}x)) dx, \\ &= \int_{\mathbb{R}^d} p(x) (\varphi(\mathbf{R}x) - \varphi(x)) dx. \end{aligned} \quad (20)$$

where $\varphi(x) = -\log p(x)$. Since KL is always non-negative, an upper bound suffices to show closeness between p and $p \circ \mathbf{R}$.

Using smoothness assumption S1 i.e. $\varphi \in C^{1,\alpha}(\mathbb{R}^d)$ with $[\nabla \varphi]_{\alpha} < \infty$, we get a Taylor-like expansion

$$\varphi(y) - \varphi(x) \leq \nabla \varphi(x) \cdot (y - x) + [\nabla \varphi]_{\alpha} \|y - x\|_2^{1+\alpha}. \quad (21)$$

for $x, y \in \mathbb{R}^d$. Setting $y = \mathbf{R}x$, and plugging (21) into (20) yields

$$\begin{aligned} &\int_{\mathbb{R}^d} p(x) (\varphi(\mathbf{R}x) - \varphi(x)) dx \\ &\leq \int_{\mathbb{R}^d} \nabla \varphi(x) \cdot (\mathbf{R}x - x) p(x) dx + [\nabla \varphi]_{\alpha} \int_{\mathbb{R}^d} \|\mathbf{R}x - x\|_2^{1+\alpha} p(x) dx \end{aligned} \quad (22)$$

The second term can be handled as

$$\begin{aligned}
\int_{\mathbb{R}^d} \|\mathbf{R}x - x\|_2^{1+\alpha} p(x) dx &\leq \|\mathbf{I} - \mathbf{R}\|_{\text{op}}^{1+\alpha} \int_{\mathbb{R}^d} \|x\|_2^{1+\alpha} p(x) dx \\
&= \|\mathbf{I} - \mathbf{R}\|_{\text{op}}^{1+\alpha} \mathbb{E}_{X \sim p} \|X\|_2^{1+\alpha} \\
&\leq \|\mathbf{I} - \mathbf{R}\|_{\text{op}}^{1+\alpha} \left(\mathbb{E}_{X \sim p} \|X\|_2^2 \right)^{\frac{1+\alpha}{2}} \\
&= \|\mathbf{I} - \mathbf{R}\|_{\text{op}}^{1+\alpha} (\text{tr } \boldsymbol{\Sigma})^{\frac{1+\alpha}{2}},
\end{aligned}$$

since $1 + \alpha \leq 2$. The first term in (22), on the other hand, is non-positive. To see this, we use the identity $\nabla p(x) = -\nabla \varphi(x) p(x)$, followed by integration-by-parts to get

$$\begin{aligned}
\int_{\mathbb{R}^d} \nabla \varphi(x) \cdot (\mathbf{R}x - x) p(x) dx &= \int_{\mathbb{R}^d} -\nabla p(x) \cdot (\mathbf{R}x - x) dx \\
&= \int_{\mathbb{R}^d} p(x) \nabla \cdot (\mathbf{R} - \mathbf{I})x dx \\
&= \int_{\mathbb{R}^d} p(x) \text{tr}(\mathbf{R} - \mathbf{I}) dx = \text{tr}(\mathbf{R}) - \text{tr}(\mathbf{I}).
\end{aligned}$$

The boundary term in the integration-by-parts is zero because $\|p(x)(\mathbf{R} - \mathbf{I})x\|_2 \rightarrow 0$ as $\|x\|_2 \rightarrow \infty$. But note that for any orthogonal \mathbf{R} ,

$$\text{tr}(\mathbf{R}) = \sum_{i=1}^d e_i \cdot \mathbf{R}e_i \leq \sum_{i=1}^d \|e_i\|_2 \|\mathbf{R}e_i\|_2 = d = \text{tr}(\mathbf{I}),$$

where e_1, \dots, e_d are the standard basis vectors in \mathbb{R}^d .

Putting these bounds together and using the inequality $\text{tr } \boldsymbol{\Sigma} \leq d \|\boldsymbol{\Sigma}\|_{\text{op}}$ gives the desired result. \square

A.5 Proof of Theorem 3.11

Theorem. Let p be a zero-mean probability density on \mathbb{R}^d , satisfying Smoothness assumption S2. Let $\mathbf{A} \in \mathbb{R}^{d \times d}$ be invertible with $\|\mathbf{A}^{-1}\|_{\text{op}} \leq B$. Then,

$$\text{TV}(p, \mathbf{A}_{\#} p) \equiv \frac{1}{2} \|\mathbf{A}_{\#} p - p\|_{L^1} \leq \frac{1}{2} \left[(1 + B) \|\nabla p\|_{L^1} \sqrt{d} + d \right] \|\boldsymbol{\Sigma}\|_{\text{op}}^{1/4} \|\mathbf{I} - \mathbf{A}\|_{\text{op}}^{1/2}.$$

Proof. Let $q = \mathbf{A}_{\#} p$ be the transformed density. Consider the standard Gaussian density $g(x) = (2\pi)^{-d/2} e^{-\frac{1}{2}\|x\|_2^2}$ on \mathbb{R}^d , and for any $\epsilon > 0$ (to be fixed later), denote the scaled version by $g_\epsilon(x) = \epsilon^{-d} g(x/\epsilon)$. We can decompose

$$\|q - p\|_{L^1} \leq \|q - q * g_\epsilon\|_{L^1} + \|q * g_\epsilon - p * g_\epsilon\|_{L^1} + \|p * g_\epsilon - p\|_{L^1}. \quad (23)$$

To bound the second term of (23), we need the following lemmas.

Lemma A.1 (L^1 bound on smoothed densities). *Let p and q be probability densities on \mathbb{R}^d , and denote by $W_1(p, q)$ the Wasserstein-1 distance between them. For any $\epsilon > 0$, it holds that*

$$\|p * g_\epsilon - q * g_\epsilon\|_{L^1} \leq \sup_{\substack{s, t \in \mathbb{R}^d \\ s \neq t}} \frac{\|\tau_s g_\epsilon - \tau_t g_\epsilon\|_{L^1}}{\|s - t\|_2} W_1(p, q),$$

where $\tau_s h(x) := h(x - s)$ denotes a translation for any function h on \mathbb{R}^d .

Proof of Lemma A.1. Denote by $\Gamma(p, q)$ the set of all couplings (or transport plans) between p and q , and let $\gamma \in \Gamma(p, q)$. Note that one can express

$$\begin{aligned}
p * g_\epsilon(x) - q * g_\epsilon(x) &= \int_{\mathbb{R}^d} g_\epsilon(x - s) p(s) ds - \int_{\mathbb{R}^d} g_\epsilon(x - t) q(t) dt \\
&= \int_{\mathbb{R}^d \times \mathbb{R}^d} (g_\epsilon(x - s) - g_\epsilon(x - t)) d\gamma(s, t).
\end{aligned}$$

A direct calculation involving an exchange of integrals and a Holder bound gives

$$\begin{aligned}
\|p * g_\epsilon - q * g_\epsilon\|_{L^1} &= \int_{\mathbb{R}^d} |p * g_\epsilon(x) - q * g_\epsilon(x)| dx \\
&\leq \int_{\mathbb{R}^d} \int_{\mathbb{R}^d \times \mathbb{R}^d} |g_\epsilon(x-s) - g_\epsilon(x-t)| d\gamma(s,t) dx \\
&= \int_{\mathbb{R}^d \times \mathbb{R}^d} \int_{\mathbb{R}^d} |\tau_s g_\epsilon(x) - \tau_t g_\epsilon(x)| dx d\gamma(s,t) \\
&= \int_{\mathbb{R}^d \times \mathbb{R}^d} \|\tau_s g_\epsilon - \tau_t g_\epsilon\|_{L^1} d\gamma(s,t) \\
&= \int_{\mathbb{R}^d \times \mathbb{R}^d} \frac{\|\tau_s g_\epsilon - \tau_t g_\epsilon\|_{L^1}}{\|s-t\|_2} \|s-t\|_2 d\gamma(s,t) \\
&\leq \sup_{\substack{s,t \in \mathbb{R}^d \\ s \neq t}} \frac{\|\tau_s g_\epsilon - \tau_t g_\epsilon\|_{L^1}}{\|s-t\|_2} \int_{\mathbb{R}^d \times \mathbb{R}^d} \|s-t\|_2 d\gamma(s,t).
\end{aligned}$$

Taking an infimum over all $\gamma \in \Gamma(p, q)$ gives the desired result. \square

Lemma A.2 (Translational stability of Gaussian kernels in L^1). *Let $s, t \in \mathbb{R}^d$, and $\epsilon > 0$. Then,*

$$\|\tau_s g_\epsilon - \tau_t g_\epsilon\|_{L^1} \leq \frac{\sqrt{d}}{\epsilon} \|s-t\|_2.$$

Proof of Lemma A.2. Fix some $x \in \mathbb{R}^d$ and consider the smooth function $[0, 1] \ni \xi \mapsto g_\epsilon(x-s+\xi(s-t))$ where ξ linearly interpolates between $x-s$ and $x-t$. This lets us write

$$g_\epsilon(x-t) - g_\epsilon(x-s) = \int_0^1 \nabla g_\epsilon(x-s+\xi(s-t)) \cdot (s-t) d\xi.$$

Integrating, we get that

$$\begin{aligned}
\int_{\mathbb{R}^d} |g_\epsilon(x-t) - g_\epsilon(x-s)| dx &\leq \int_{\mathbb{R}^d} \int_0^1 \|\nabla g_\epsilon(x-s+\xi(s-t))\|_2 \|s-t\|_2 d\xi dx \\
&\leq \int_0^1 \|s-t\|_2 \int_{\mathbb{R}^d} \|\nabla g_\epsilon(x-s+\xi(s-t))\|_2 dx d\xi \\
&= \int_{\mathbb{R}^d} \|\nabla g_\epsilon(x)\|_2 dx \|s-t\|_2.
\end{aligned}$$

What remains is to bound the integral $\int_{\mathbb{R}^d} \|\nabla g_\epsilon(x)\|_2 dx$, and this is straightforward. Noting that

$$\frac{\partial g_\epsilon}{\partial x_j}(x) = -\frac{x_j}{\epsilon^2} g_\epsilon(x),$$

we get

$$\int_{\mathbb{R}^d} \|\nabla g_\epsilon(x)\|_2 dx = \frac{1}{\epsilon^2} \int_{\mathbb{R}^d} \|x\|_2 g_\epsilon(x) dx = \frac{1}{\epsilon^2} \mathbb{E}_{X \sim N(0, \epsilon^2)} \|X\|_2 \leq \frac{\sqrt{d}}{\epsilon},$$

which completes the proof of the lemma. \square

Together, these lemmas give that

$$\|q * g_\epsilon - p * g_\epsilon\|_{L^1} \leq \frac{\sqrt{d}}{\epsilon} W_1(q, p). \quad (24)$$

The right-hand side is now a problem of stability in the Wasserstein-1 distance, and is handled in the following lemma.

Lemma A.3 (Stability in W_1). *Let p be a probability density on \mathbb{R}^d with mean zero and covariance matrix Σ , and let $\mathbf{A} \in \mathbb{R}^{d \times d}$. Then,*

$$W_1(\mathbf{A} \# p, p) \leq \sqrt{\text{tr}(\Sigma)} \|\mathbf{A} - \mathbf{I}\|_{\text{op}}.$$

Proof of Lemma A.3. A direct calculation yields

$$\begin{aligned}
W_1(\mathbf{A}_\# p, p) &\leq \inf_{\substack{T: \mathbb{R}^d \rightarrow \mathbb{R}^d \\ \text{measurable}}} \left\{ \int_{\mathbb{R}^d} \|T(x) - x\|_2 p(x) dx : T_\# p = \mathbf{A}_\# p \right\} \\
&\leq \int_{\mathbb{R}^d} \|\mathbf{A}x - x\|_2 p(x) dx \\
&\leq \|\mathbf{I} - \mathbf{A}\|_{\text{op}} \int_{\mathbb{R}^d} \|x\|_2 p(x) dx \\
&\leq \|\mathbf{I} - \mathbf{A}\|_{\text{op}} \mathbb{E}_{X \sim p} \|X\|_2.
\end{aligned}$$

The result then follows because $\mathbb{E}\|X\|_2 \leq \sqrt{\mathbb{E}\|X\|_2^2} = \sqrt{\text{tr}(\boldsymbol{\Sigma})}$. \square

Noting that $\text{tr}(\boldsymbol{\Sigma}) \leq \|\boldsymbol{\Sigma}\|_{\text{op}} d$, Lemma A.3 together with (24) give the bound

$$\|q * g_\epsilon - p * g_\epsilon\|_{L^1} \leq \frac{d}{\epsilon} \|\boldsymbol{\Sigma}\|_{\text{op}}^{1/2} \|\mathbf{I} - \mathbf{A}\|_{\text{op}},$$

which concludes the analysis of the second term of (23). Now, we handle the first and third terms of (23), making use of the assumed smoothness (S2) of p .

Lemma A.4 (L^1 error due to mollification). *Let p be a probability density on \mathbb{R}^d satisfying Smoothness assumption S2. Then, for any $\epsilon > 0$,*

$$\|p * g_\epsilon - p\|_{L^1} \leq \|\nabla p\|_{L^1} \sqrt{d} \epsilon.$$

Proof of Lemma A.4. We first relate the approximation error above to the translational stability in L^1 :

$$\begin{aligned}
\|p * g_\epsilon - p\|_{L^1} &= \int_{\mathbb{R}^d} \left| \int_{\mathbb{R}^d} (p(x-y) - p(x)) g_\epsilon(y) dy \right| dx \\
&\leq \int_{\mathbb{R}^d} \int_{\mathbb{R}^d} |\tau_y p(x) - p(x)| dx g_\epsilon(y) dy \\
&= \int_{\mathbb{R}^d} \|\tau_y p - p\|_{L^1} g_\epsilon(y) dy.
\end{aligned}$$

This translational stability $\|\tau_y p - p\|_{L^1}$ is controlled via smoothness. Suppose first that $p \in \mathcal{C}^1(\mathbb{R}^d)$, so that for $x, y \in \mathbb{R}^d$,

$$p(x-y) - p(x) = \int_0^1 \nabla p(x - \xi y) \cdot (-y) d\xi.$$

Integrating gives

$$\begin{aligned}
\|\tau_y p - p\|_{L^1} &\leq \int_{\mathbb{R}^d} \int_0^1 \|\nabla p(x - \xi y)\|_2 \|y\|_2 d\xi dx \\
&= \int_0^1 \|y\|_2 \int_{\mathbb{R}^d} \|\nabla p(x - \xi y)\|_2 dx d\xi \\
&= \int_{\mathbb{R}^d} \|\nabla p(x)\|_2 dx \|y\|_2 = \|\nabla p\|_{L^1} \|y\|_2.
\end{aligned}$$

If $p \notin \mathcal{C}^1(\mathbb{R}^d)$, one can use the fact that p lives in the Sobolev space $\mathcal{W}^{1,1}(\mathbb{R}^d)$ to get an approximating sequence $p_k \in \mathcal{C}^1(\mathbb{R}^d) \cap \mathcal{W}^{1,1}(\mathbb{R}^d)$ satisfying $\|p_k - p\|_{L^1} \rightarrow 0$ and $\|\nabla p_k - \nabla p\|_{L^1} \rightarrow 0$ [24]. This allows us to extend the bound

$$\|\tau_y p - p\|_{L^1} \leq \|\nabla p\|_{L^1} \|y\|_2$$

to all $p \in \mathcal{W}^{1,1}(\mathbb{R}^d)$. Combining, we get

$$\|p * g_\epsilon - p\|_{L^1} \leq \int_{\mathbb{R}^d} \|\tau_y p - p\|_{L^1} g_\epsilon(y) dy \leq \|\nabla p\|_{L^1} \int_{\mathbb{R}^d} \|y\|_2 g_\epsilon(y) dy \leq \|\nabla p\|_{L^1} \sqrt{d} \epsilon.$$

\square

Lemma A.4 directly bounds the third term of (23). To address the first term, we apply Lemma A.4 to $q(x) = |\det \mathbf{A}^{-1}| p(\mathbf{A}^{-1}x)$, noting that $\|\nabla q\|_{L^1} \leq \|\mathbf{A}^{-1}\|_{\text{op}} \|\nabla p\|_{L^1}$. This finally yields the bound

$$\|q - p\|_{L^1} \leq (1 + \|\mathbf{A}^{-1}\|_{\text{op}}) \|\nabla p\|_{L^1} \sqrt{d} \epsilon + \frac{d}{\epsilon} \|\Sigma\|_{\text{op}}^{1/2} \|\mathbf{I} - \mathbf{A}\|_{\text{op}}.$$

The following choice completes the proof of Theorem 3.11.

$$\epsilon = \|\Sigma\|_{\text{op}}^{1/4} \|\mathbf{I} - \mathbf{A}\|_{\text{op}}^{1/2}.$$

□

B Computational details and further numerical results

B.1 Monte Carlo integration for computing squared Hellinger distances

Recall that the squared Hellinger between densities p and q on \mathbb{R}^d is defined by the integral

$$h_d^2(p, q) := \frac{1}{2} \int_{\mathbb{R}^d} \left(\sqrt{q(x)} - \sqrt{p(x)} \right)^2 dx. \quad (25)$$

If d is larger than 4, computing the integral by discretizing on a grid can prove prohibitively expensive. Instead, one can use simple Monte Carlo integration to approximate (25). Notice that

$$h_d^2(p, q) = \frac{1}{2} \int_{\mathbb{R}^d} \left(\sqrt{q(x)/p(x)} - 1 \right)^2 p(x) dx = \mathbb{E}_{X \sim p} \frac{1}{2} \left(\sqrt{q(X)/p(X)} - 1 \right)^2,$$

where the expectation on the right-hand side can be approximated using an empirical average. We simulate samples $S^{(1)}, S^{(2)}, \dots, S^{(K)} \stackrel{\text{iid}}{\sim} p$, and compute

$$\frac{1}{K} \sum_{k=1}^K \frac{1}{2} \left(\sqrt{q(S^{(k)})/p(S^{(k)})} - 1 \right)^2$$

which converges almost surely to $h_d^2(p, q)$ as $K \rightarrow \infty$. In practice, we use $K = 10000$. Additionally, we repeat the procedure 50 times and ensure that the resulting spread is not too large.

B.2 The EM algorithm and the re-sampling heuristic

Recall the finite mixture densities discussed in Section 4.3

$$p(x) = \sum_{k=1}^K \pi_k p_k(x),$$

and consider samples $X^{(1)}, X^{(2)}, \dots, X^{(n)} \stackrel{\text{iid}}{\sim} p$. We briefly describe the EM algorithm following Cule et al. [9]. Given current iterates of the mixture proportions $\tilde{\pi}_1, \dots, \tilde{\pi}_K$ and component densities $\tilde{p}_1, \dots, \tilde{p}_K$, compute the posterior probabilities

$$\tilde{\theta}_{jk} \leftarrow \frac{\tilde{\pi}_k \tilde{p}_k(X^{(j)})}{\sum_{\ell=1}^K \tilde{\pi}_\ell \tilde{p}_\ell(X^{(j)})}. \quad (26)$$

Then, for each component $k \in \{1, \dots, K\}$, update the density \tilde{p}_k by maximizing a weighted likelihood over a suitable class of densities \mathcal{F} (such as log-concave densities):

$$\tilde{p}_k \leftarrow \arg \max_{q_k \in \mathcal{F}} \sum_{j=1}^n \tilde{\theta}_{jk} \log q_k(X^{(j)}). \quad (27)$$

Finally, update the mixture proportions as

$$\tilde{\pi}_k \leftarrow \frac{1}{n} \sum_{j=1}^n \tilde{\theta}_{j,k} \quad (28)$$

for each k . These three steps can be iterated until convergence.

When combining the EM algorithm with LC-IC, (26) and (28) remain unchanged. Only the maximum likelihood step (27) needs to be replaced, where one needs to “fit” a density to samples weighted by $\tilde{\theta}_{jk}$. Since weighted samples are not immediately compatible with our sample splitting scheme, we propose the following heuristic re-sampling scheme. From the observed samples $X^{(1)}, X^{(2)}, \dots, X^{(n)}$, construct the weighted empirical distribution

$$\tilde{\nu}_k := \frac{\sum_{j=1}^n \tilde{\theta}_{jk} \delta_{X^{(j)}}}{\sum_{j=1}^n \tilde{\theta}_{jk}}$$

for each k . Notice that $\tilde{\nu}_k$ depends on the current iterates. Next, (computationally) generate iid samples from $\tilde{\nu}_k$ (hence the term *re-sampled*), and feed them into Algorithm 1, using M of those re-sampled samples for the unmixing matrix estimation stage, and N for the marginal estimation stage. The output of Algorithm 1 is then the updated iterate of \hat{p}_k . Unlike the sample splitting scheme discussed before, the re-sampling heuristic involves no compromise between M and N ; one can generate as many samples from $\tilde{\nu}_k$ as they like. The experiments in Section 4.3 used $N = M = 4n$.

However, it is important to note that we do not have a theoretical backing for this heuristic yet. Another issue in this strategy is the generation of spuriously zero values of $\tilde{\theta}_{jk}$, which can cause division-by-zero errors and likelihoods of $-\infty$. We address this by adding a small positive number such as 10^{-7} to the zero values of $\tilde{\theta}_{jk}$.

B.3 Comparison of performance on Gamma-distributed data

Here, we repeat the experiments from Section 4.1, but for Gamma distributed data. Consider the bivariate case first. Let $X = \mathbf{W}^T Z$ with $\mathbf{W} = \mathbf{I}$ and $Z = (Z_1, Z_2)$, such that $Z_1 \sim \text{Gamma}(6, 1)$ and $Z_2 \sim \text{Gamma}(3, 1)$. With $n = 1000$ iid samples of X generated, equally split $M = N = 500$, and compute the LC-IC estimate using PCA for unmixing matrix estimation and `logcondens` for marginal estimation. From the same $n = 1000$ samples, also compute the LC-MLE estimate with `LogConcDEAD`. Figure 6 shows the ground truth and estimated densities together with their contour plots, and lists the estimation errors in squared Hellinger distance along with the algorithm runtimes.

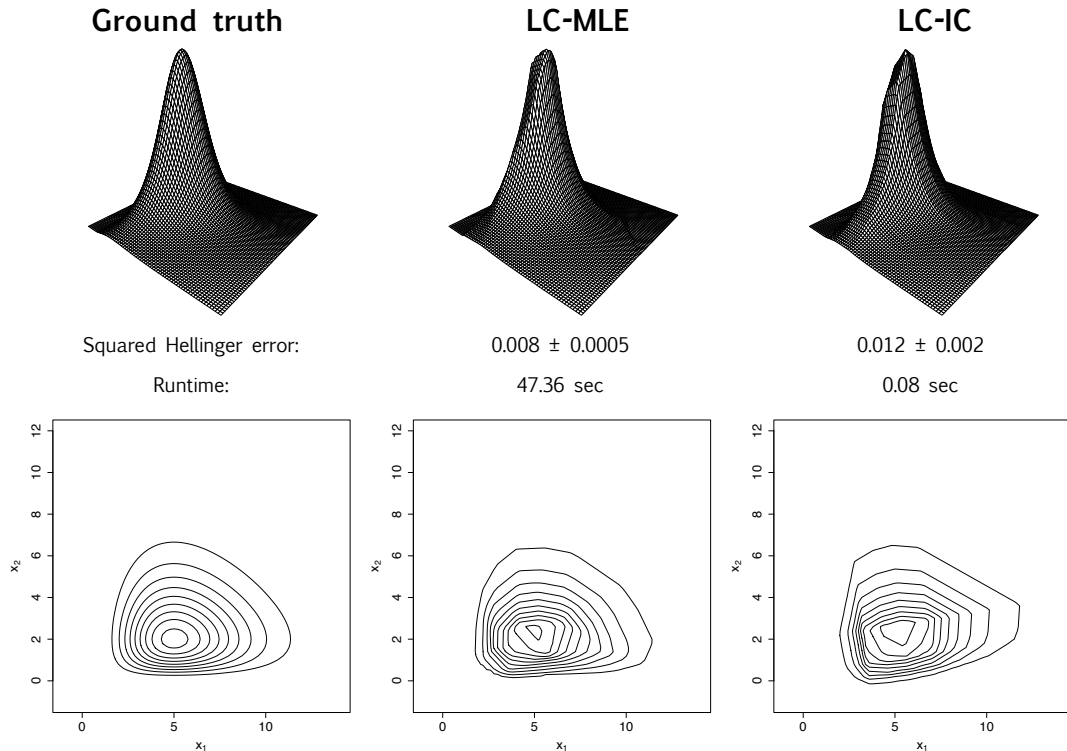


Figure 6: Comparing density estimation performance of LC-IC with LC-MLE on simulated Gamma-distributed data in $d = 2$. The ground truth and estimated densities are visualized in the top row, and the corresponding level curves are plotted in the bottom row.

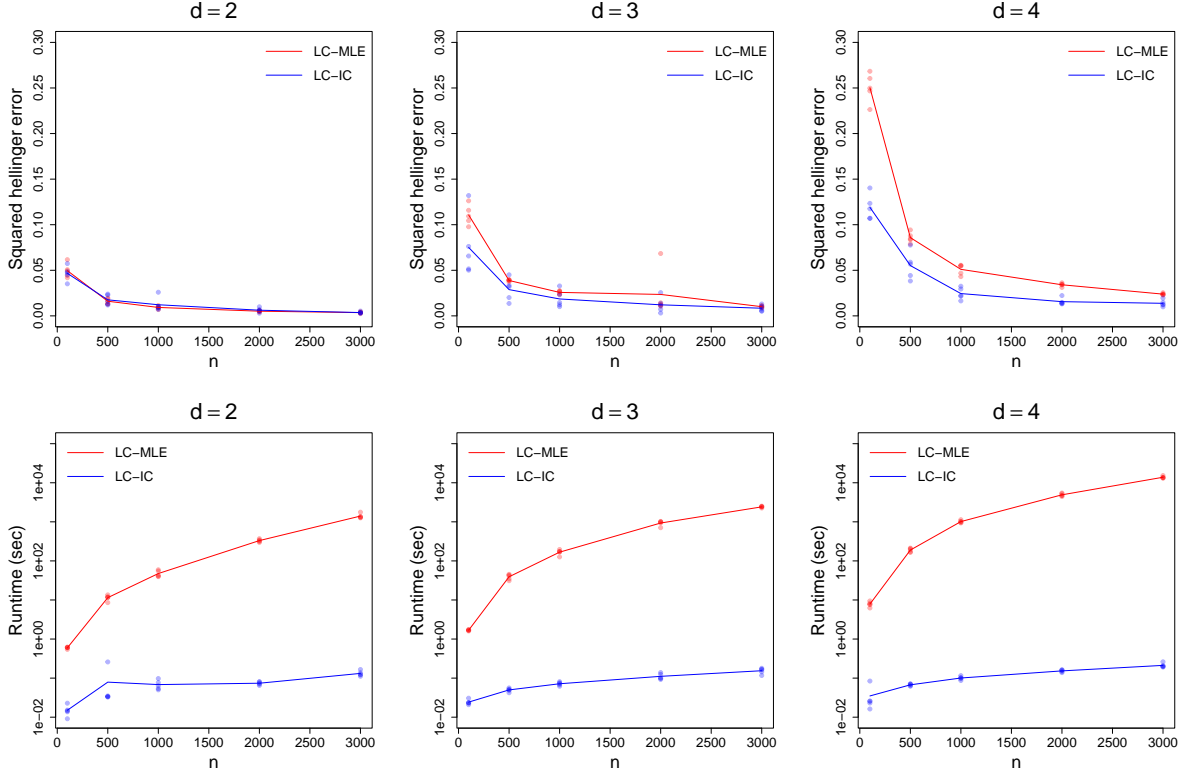


Figure 7: Comparing estimation errors in squared Hellinger distance (top row) and algorithm runtimes (bottom row) of LC-IC with LC-MLE, on simulated Gamma distributed data. The dots correspond to independent experiments, and the lines represent averages. Here, n is the number of samples, and d is the dimension.

Finally, we conduct systematic tests similar to Section 4.1 for $d = 2, 3, 4$ and various n . Set $X = \mathbf{W}^T Z$, where $\mathbf{W} = \mathbf{I}$ and $Z = (Z_1, \dots, Z_d)$, with $Z_i \sim \text{Gamma}(6 - (i - 1), 1)$. PCA is used for estimating \mathbf{W} . Each experiment is repeated 5 times, and the average metrics are computed. Figure 7 plots the estimation errors in squared Hellinger distance, as well as the algorithm runtimes, for both LC-MLE and LC-IC. The results are consistent with those from Section 4.1.